Long-term exposure to fluoride and tebuconazole alters gill, skin and gut microbiomes in rainbow trout (Oncorhynchus mykiss)

Marine Suchet
Univ. Bordeaux, CNRS, Bordeaux INP, EPOC, UMR 5805
Pauline Pannetier
Univ. Bordeaux, CNRS, Bordeaux INP, EPOC, UMR 5805
Morgane Danion
French Agency for Food, Environmental and Occupational Health & Safety
Thomas Braunbeck
University of Heidelberg
Préscillia Alves Gomes
Genome Transcriptome Platform Bordeaux (PGTB)
Jérôme Cachot
Univ. Bordeaux, CNRS, Bordeaux INP, EPOC, UMR 5805
Laure Bellec
laure.bellec@u-bordeaux.fr

Univ. Bordeaux, CNRS, Bordeaux INP, EPOC, UMR 5805

Research Article

Keywords: Aquatic pollution, aquaculture, fish, holobiont, metabarcoding, microbial ecotoxicology, symbiotoxicity

Posted Date: June 30th, 2026

DOI: https://doi.org/10.21203/rs.3.rs-9720881/v1

Additional Declarations: No competing interests reported.

Abstract

Background

. Fluoride and tebuconazole are two compounds widely used in industrial processes and agriculture, respectively, and are regularly detected in surface waters. Therefore, there is an urgent need to characterise their effects on aquatic organisms. In this context, adopting a holistic approach that integrates the host and its associated microbial communities, the holobiont, is particularly relevant. In this study, rainbow trout were exposed from 6 days post-fertilisation for 7 months to two environmental concentrations of fluoride (6.8 or 24.7 mg/L), to tebuconazole (51.7 µg/L), or maintained in control conditions. At the end of the exposure period, digestive, cutaneous and respiratory microbial communities were characterized using 16S rRNA gene metabarcoding.

Results

. Fluoride and tebuconazole significantly affected the bacterial alpha diversity in gill and skin tissues, while the beta diversity was affected across all three tissues. If compared to the control treatment, fluoride exposure altered microbial co-occurrence networks, affecting bacterial interconnections in a tissue-specific manner, with reduced interconnections in gills and increased interconnections in skin and intestine compared to the control treatment. Shifts in taxonomical composition were present following exposure to both pollutants, and notably increases in the relative abundance of fish pathogens such as *Candidatus Piscichlamydia*, *Flavobacterium* and *Aeromonas* were observed. The present study also highlighted a potential co-selection of antibiotic-resistant taxa such as *Aeromonas* and *Acidovorax*, as well as an increased expression of predicted pathways linked to antibiotic resistance following chemical exposure to fluoride and tebuconazole.

Conclusions

. These results highlight alterations of digestive, cutaneous and respiratory microbiomes in the rainbow trout following chronic exposure to fluoride and tebuconazole, with distinct and tissue-specific microbial responses. Beyond taxonomical shifts, the observed alterations of bacterial co-occurrence networks, enrichment of pathogenic bacteria, and antibiotic-resistant taxa indicate that the microbiome of fish may represent a sensitive bioindicator system of chemical stress. Such alterations might well impair host health and, under a One Health perspective, have broader implications for environmental and human health.

Background

The microbiota is defined as all the microorganisms living in an ecosystem or a particular area (1). They are involved in the digestion and metabolism of nutrients, in the development of the innate and adaptive

immune systems and in the defence against opportunistic and pathogenic bacteria (2). In humans, the gut microbiome may contain up to 150 times more genetic material than the human genome (3). In teleost fish, research on microorganisms associated with different tissues so far remained scarce compared to humans or rodents. However, recent evidence suggests that fish hosts actively shape their microbiota, with marked differentiation in microbial composition and diversity across tissues (4, 5). Two main factors contribute to shaping fish-associated microbial communities: First, environmental factors such as pH, temperature, water quality or geographic location can impact microbial communities (6–10). Second, host factors, including genetics, species, age or trophic level also influence the microbiota (11–16). Interestingly, the contribution of each type of factor to the microbial composition seems to be tissue-specific, with the gut microbiota being more sensitive to host factors and external microbial communities more sensitive to environmental ones (5, 17).

Gut-associated microbial communities have increasingly been studied in aquaculture to understand their roles in fish health and growth, and how both could be managed using pre- and probiotics (18, 19). However, research on microorganisms associated with other tissues, such as gills or skin, is scarce. These tissues exert key functions at the interface between the host and its environment, suggesting that their associated microbiome may be functionally distinct, relevant to fish health and important to study (20). Gills are the dominant site for gas exchanges, and, beyond respiration, they are also involved in osmoregulation, acid-base balance and nitrogenous waste excretion (21). The skin and the secreted epithelial mucus are involved in inter- and intraspecific interactions, osmoregulation, and are a physical and biochemical barrier against pathogens (22). The sampling of skin mucus is non-invasive, which makes the microbial community associated with this tissue a promising bioindicator of disease or water quality disturbances in aquaculture (22, 23). Among water quality disturbances, exposure to pollutants can lead to dysbiosis, i.e., an imbalance in the microbial communities (24–26). Therefore, ecotoxicological studies tend to adopt an integrative approach by considering the effects of pollutants on the holobiont, i.e., the unit formed by the host and its associated microorganisms (27). Chronic exposure to pesticides, metals, plastics, sunscreen, endocrine disruptors, etc. can result in impaired microbial diversity, taxonomical composition and interactions in fish microbiome (24, 28–32).

Fluorine is a widely distributed element, mainly occurring as fluoride (F^-) in aquatic environments, originating from both natural and anthropogenic sources (33). Natural sources include weathering of F^--rich minerals, volcanic activity or marine aerosols; and anthropogenic ones include coal combustion, phosphate processing or glass manufacturing (33–35). In unpolluted freshwaters, F^- concentrations typically range from 0.01 to 0.3 mg/L (33). In naturally enriched regions, F^- concentrations in surface water can be as high as 50 mg/L (Yellowstone springs, USA) or 69 mg/L (Mount Meru, Tanzania) (33, 36). In industrial wastewaters, they can reach 9720 mg/L and although treatment processes exist, F^- concentrations in effluents typically remain above 20 mg/L prior to environmental release (37, 38). Fluoride can help prevent dental caries and is therefore added to drinking water in many countries (39, 40). As a consequence, domestic wastewater also contributes to increasing F^- levels in aquatic environments (41). According to the World Health Organization, fluoride levels above 1.5 mg/L increase

the risk to develop dental and skeletal fluorosis in humans (34). In fish, chronic fluoride exposure can induce oxidative stress, altered energetic metabolism, osmoregulation and growth, induce teratogenic effects, as well as endocrine disruption (42–45). Two studies also highlighted gut microbiome alterations in fish following chronic F^- exposure at high concentrations (80 mg/L; 90 days) (46, 47). Fluoride in the form of sodium fluoride (NaF) was also added to List II of the European Union (EU), including “substances under evaluation for endocrine disruption under EU legislation”.

Tebuconazole (Tbz) is a triazole fungicide used in agriculture and as a biocide for the protection of materials and surfaces such as wood, paints and coatings (48). It is one of the most used fungicides worldwide, and is therefore frequently detected in the aquatic environments due to discharge of wastewater treatment plants and agricultural surface runoff (49). Tbz levels ranged from 1.4 to 160 ng/L along an urbanization gradient in the Seine river (France), accounting for inputs related to its biocidal uses (50). In agricultural contexts, concentrations can be higher: A one-year (2020) hydrogeochemical monitoring of Tbz in south-western France, carried out upstream of a pond in an agricultural catchment area, revealed an average concentration of 624 ± 255 ng/L and a maximum value of 6703 ng/L (51). Tbz concentrations can reach 81 µg/L in runoff waters during the first rainfall following fungicide application (52). On the other hand, Tbz exposure can exert harmful effects on aquatic organisms: Chronic exposure of fish can induce oxidative stress, hepatotoxicity, trigger apoptosis, disrupt the energetic balance and swimming behavior, and exert teratogenic as well as endocrine disrupting effects (53–57). A recent study also highlighted disruption in gut microbial communities in Japanese medaka following Tbz exposure (1 mg/L; 60 days) (58).

The rainbow trout (*Oncorhynchus mykiss*) is both a model species in ecotoxicology and a key species for aquaculture, with approximately 738.5 k tons produced worldwide in 2020 according to the Food and Agriculture Organization of the United Nations (59). As it develops in freshwater, it is exposed to pollutants such as fluoride and tebuconazole. While a few studies have been published on acute and sublethal effects of these pollutants on rainbow trout (60–62), none considered effects on the rainbow trout microbiome. Additionally, to assess the effects of pollutants, studies mainly rely on an exposure design where organisms are continuously exposed. However, realistic environmental exposure conditions are intermittent as pollutants inputs in aquatic ecosystems depend on discharges, runoffs or rainfall events (63, 64). The effects of pollutants may, however, differ significantly between continuous and intermittent exposure scenarios (64–67).

The aim of the present study was to determine the impact of chronic fluoride or tebuconazole exposure on the rainbow trout gill, skin and gut bacterial communities. For this end, rainbow trout were exposed from 6 days post-fertilization for 7 months to fluoride (6.8 or 24.7 mg/L), tebuconazole (51.7 µg/L), or maintained under control conditions. Microbiome analyses were performed to assess whether fluoride or tebuconazole exposure could (i) alter the diversity and structure of bacterial communities; (ii) induce tissue-specific effects; (iii) change the relative abundance and taxonomical composition among treatments. Finally, under a One Health perspective, we discuss how microbiome perturbations might lead to risks for host, environmental and human health.

Methods

Ethics requirements

Experimentations realised in this study were validated by an aggregated institutional review board, i.e., an animal ethics committee, ANSES/ENVA/UPEC N°16 and authorised by the French Ministry of National Education, Higher Education and Research under the number APAFIS#39732-2022112416434185 v7. Fish anaesthesia method, realised by an immersion in 20 ppm eugenol (CAS no. 97-53-0, FiliaVet France) bath, and euthanasia method, realised by a swift transection of the brainstem, inducing immediate loss of consciousness followed by death were reviewed and approved by the same national committees.

Experimental conditions and chemical exposure

The rainbow trout (*Oncorhynchus mykiss*) used in this study were sourced from the in-house breeding stock maintained at the ANSES Laboratory fish rearing facilities in Plouzané, France. These fish are bred and reared on-site under controlled, specific pathogen-free conditions as part of the laboratory's permanent aquatic animal facility, and no external supplier was involved in their provision. In November 2023, ten adults rainbow trout (*Oncorhynchus mykiss*) were selected for reproduction. Fish were anesthetized in a 20 ppm eugenol bath before being gently stripped to collect eggs and sperm. Fertilized eggs were then randomly distributed in each aquarium (12L; 210 embryos/ aquarium; 1 aquarium /treatment) and at the end of the larval stage, 90 randomly selected fish per experimental treatment were transferred to 50 L aquaria in the same room with identical physicochemical water parameters (68). Water temperature was thermoregulated at 12.41 ± 0.54°C during the duration of the experiment and water physicochemical parameters were monitored periodically [additional file 1, table S1].

Rainbow trout were exposed from 6 days post-fertilization (dpf) during 7 months, to four different chemical treatments: a non-exposed control; tebuconazole at 51.7 µg/L (Tbz; CAS no. 107534-96-3; Sigma-Aldrich); and two concentrations of fluoride, F1 (6.8 mg F^-/L) and F2 (24.7 mg F^-/L) (68). Fluoride exposure was achieved using sodium fluoride (NaF; CAS no. 7681-49-4, Sigma-Aldrich) as the source compound, but concentrations were quantified and expressed as fluoride concentrations (mg F^-/L). Trout were exposed 7 hours per day, freshwater flow was stopped during the daily exposure period, before being restored for the rest of the day, allowing gradual dilution. Stock solutions of pollutants were stored at room temperature, in the dark and renewed weekly. The fluoride stock solution (19.2 g F^-/L) was prepared by diluting NaF in pure water and added directly to the aquaria each morning. The tebuconazole stock solution was prepared by dissolving 250 mg in 10 mL DMSO (CAS no. 67-68-5, Sigma-Aldrich), before being diluted in ultrapure water to obtain a 20.6 mg/L working solution (0.082% DMSO) and added directly to the aquaria each morning. Fluoride and tebuconazole concentrations were measured, by an external service provider (LABOCEA, France) [additional file 1, table S2].

Sampling

All samples were collected on the same day (06/06/2024) under a biological safety cabinet, with a laminar flow hood and using sterile instruments. From each aquarium, 1 L of water was collected and divided into three replicates, which were then filtered using a filtration unit onto 0.22 µm sterile membranes (Grosseron SAS, France). Sterile membranes were stored at -80°C until DNA extraction. Fish were then collected, approximately 15 hours after the last feeding, to avoid the presence of food in the digestive tract. Fish were euthanized by a swift transection of the brainstem, posterior to the head, at the level of the spinal canal, inducing immediate loss of consciousness followed by death. They were weighed, measured (standard length, i.e., from the tip of the mouth to the base of the caudal fin), and their Fulton index was calculated (69). Epidermal mucus, gills and midgut were sampled from each trout for each treatment condition (N = 10–12 per treatment [see additional file 1, table S3]). Epidermal mucus, i.e., skin, was collected on sterile DryTransport swabs with Hydraflock tips (Dominique Dutscher SAS, France) by performing ten gentle strokes along the left side of the fish, above the lateral line, starting behind the head and ending just before the caudal fin. Swabs were stored at -80°C until DNA extraction. For gill samples, the four gill arches on the left side of the fish were dissected, flash-frozen in liquid nitrogen and stored at -80°C until DNA extraction. For midgut samples, i.e., intestine, an approximately 2 cm section was collected downstream from the pyloric caeca, and at least 2 cm upstream from the urogenital opening to limit the risk of collecting hindgut sections. Intestine samples were then flash-frozen in liquid nitrogen and stored at -80°C until DNA extraction.

Sex identification

The age of the trout at sampling (7 months) did not allow visual determination of the sex. Sex was determined using a PCR targeting the *sdy* gene, a male-specific locus (70). Each 25 µL reaction contained 2 µL gill DNA, 5 µL 5X Green GoTaq® Flexi Buffer (Promega), 0.5 µL nucleotide mix (10 mM), 2 µL $MgCl_2$ (25 mM), 1 µL specific primers (20µM; *sdy*-F: 5'-GTTCATATGCCAGGCTCAAC-3'; *sdy*-R: 5'-CGATTAGAAAGGCCTGCTTG-3'), 0.125 µL GoTaq® G2 Flexi DNA polymerase (5 U/µL) and DNase free water. PCR reactions were carried out using a Mastercycler® Nexus (Eppendorf): 94°C for 3 min, followed by 30 cycles (94°C for 30 s; 63°C for 30 s; 72°C for 1 min), and finally 72°C for 7 min. A control PCR was performed on each sample targeting the *actβ* gene (*actβ*-F: 5'- TGTGGATCAGCAAGCAGGAG-3'; *actβ*-R: 5'- CAGCCTTCACAGAGGCAAAT-3') following the same conditions except hybridization temperature (60°C). Absence of amplification of *sdy* and positive amplification of *actβ* indicated females, while positive amplification of *sdy* and *actβ* indicated males [see additional file 1, table S3].

DNA extraction and sequencing

DNA extraction and sequencing were done according to Bellec, Le Du-Carreet al.,, 2022 (28) with a few modifications. DNA from water samples was extracted using the Qiagen® DNeasy PowerWater kit, DNA from intestine samples was extracted using the Qiagen® QIAamp DNA Mini Kit and DNA from gills and skin samples was extracted using the Qiagen® QIAamp PowerFecal Pro kit, following the manufacturer's instructions. DNA samples were then sent to the Genome Transcriptome Platform Bordeaux

(www.pgtb.fr, Cestas Pierroton, France) for library preparation and sequencing. Sequencing was performed on 450 bp fragments of the 16S rRNA gene, V3-V4 region, to target bacterial communities (341-F: 5'-CCTACGGGNGGCWGCAG-3'; 785-R: 5'-GACTACHVGGGTATCTAATCC-3') (71). Sequencing was performed on an Illumina NextSeq2000 using a 2 x 300 cycle flow cell with a NextSeq 1000/2000 P2 XLEAP-SBS Reagents kit (Illumina). Negative controls and positive bacterial mock community controls (ZymoBIOMICS Microbial Community DNA Standard, Zymo Research) were also used for amplification and sequencing.

Bioinformatic processing

After sequencing, 16S rRNA gene reads were bioinformatically processed using the FROGS v5 pipeline (72). First of all, a denoising step was performed, sequences > 300 bp were removed before being depleted of primers using Cutadapt v2.10 with a maximum error rate of 0.1. Sequences lacking primers were discarded. Next, the vsearch tool (v2.17.0) was used to merge forward and reverse sequences with a maximum mismatch rate of 0.05 (73). Amplicons between 320 and 600 bp were retained, and Amplicon Sequence Variants (ASVs) were generated using the DADA2 process with independent sample inference (74). Chimeras were removed using vsearch. Additionally, an abundance filter was applied to ASVs, with a threshold of 0.005% (75). ASVs were taxonomically assigned by BLASTN (76) and RDP (77) with SILVA v138.2 reference database (78, 79). Only taxonomic assignations with an RDP bootstrap confidence > 0.8 and BLAST alignments showing at least 90% coverage and 97% identity were kept. Finally, contaminant sequences were identified and removed using the R package microDecon (v1.0.2), which corrects for contaminations based on negative control samples (80). The decon function was run using the default parameters (runs = 2; thresh = 0.7; prop.thresh = 0.00005). The phyloseq package (v1.52.0) (81) was used for further analyses.

Statistical analysis

Statistical analyses and data visualizations were performed using R software (version 4.5.1, www.r-project.org). Alpha diversity statistical comparisons were done using the Wilcoxon rank-sum test (between matrices and sex), the Wilcoxon signed-rank test for matched samples (among tissues) or using a one-way ANOVA, followed by a Tukey post-hoc (among chemical treatments). Beta diversity analyses were performed on Bray-Curtis dissimilarity matrices, after Cumulative Sum Scaling (CSS) normalization using the metagenomeSeq R package (82) and were visualized using Principal Coordinate Analysis (PCoA). Beta dispersion was compared using a multivariate homogeneity of group dispersions test (1000 permutations). Beta diversity was compared between groups by permutational multivariate analysis of variance (PERMANOVA; 999 permutations) using the adonis2 function of the vegan R package (83), and multilevel comparisons were performed using the pairwiseAdonis R package (84).

Microbial analyses

A differential analysis was performed as implemented in the DESeq2 R package (v1.48.1) (85), and results were considered significant if p-value < 0.01. Venn diagrams, indicating shared and unique ASV among treatments and tissues, were generated using the ggVennDiagram R package (v1.5.4) (86).

Bacterial microbiomes co-occurrence networks were generated using sparse inverse covariance estimation for ecological association (SPIEC-EASI; SpiecEasi R package (v1.1.1); Kurtz, Mulleret al.,, 2015 (87)). Before inference, ASVs with relative abundance < 0.01% were removed. Networks were then inferred with SPIEC-EASI using the Meinhausen-Bühlmann neighbourhood selection (method = “mb”) and stability selection via StARS (sel.criterion = “stars”) with 99 pulsar repetitions. The resulting adjacency matrix (refit) was converted to an igraph object for further calculations (igraph R package (v2.1.4); Csardi and Nepusz, 2006 (88)). Node sizes were scaled by degree, and network modules were detected using the Louvain algorithm. The network visualization was plotted with a Fruchterman-Reingold layout (seed set for reproducibility).

Functional predictions were generated from 16S rRNA data using PICRUSt2 (Phylogenetic Investigation of Communities by Reconstruction of Unobserved States; Douglas, Maffeiet al.,, 2020 (89)) with default parameters. The workflow included phylogenetic placement of ASVs using EPA-NG (Evolutionary Placement Algorithm Next Generation; Barbera, Kozlovet al.,, 2019 (90)), hidden-state prediction with GAPPA (Genetic Ancestral Prediction and Parsimony Analysis; Czech, Barberaet al.,, 2020 (91)), gene family prediction and pathway reconstruction using MinPath (Minimal Set of Pathways; Ye and Doak, 2009 (92)). Results were filtered to remove ASVs with a Nearest Sequenced Taxon Index (NSTI) value > 0.5 to ensure higher confidence in functional prediction. Finally, MetaCyc functional pathways were compared among treatments using DESeq2, according to the same methods as described previously, but only pathways with a $\log_2$ fold change < -1 or > 2 were retained.

Results

Rainbow trout mortality and growth

Trout mortality was recorded each day. Mortality during the embryonic and larval stages (fertilization to 788 degree days) was 17.3%, 10.5%, 7.3% and 11.2% in the Control, F1, F2 and Tbz treatments, respectively [see additional file 2, Figure S1A]. During the juvenile stage (788 degree days to the end of the experiment), mortality was 4.6%, 8.6%, 3.6% and 8.5%, respectively [see additional file 2, Figure S1B]. At the sampling day, each fish was weighed, measured, and its Fulton index was calculated. Mean (± std) length was 18.0 ± 1.1 cm, mean weight was 71.5 ± 13.4 g, and mean Fulton index was 1.22 ± 0.09 [see additional file 2, Figure S1C]. No statistical differences were highlighted among exposure treatments.

Sequencing and ASV processing

A total of 34,606,774 reads were produced after sequencing of 138 *Oncorhynchus mykiss* individuals, 12 water samples, 23 blanks and 5 positive controls [see additional file 1, table S4]. Seven extraction blanks and 16 PCR blanks were included and represented 1,236,403 reads (3.6%). Five positive controls, i.e.,

mock communities, were included to ensure the quality of sequencing and affiliation. These samples produced 702,899 reads, and their taxonomical profiles matched the theoretical composition provided by the manufacturer. Blanks were used to filter out contaminant sequences, and reads corresponding to chloroplasts or non-affiliated at the phylum, class or order taxonomical levels were removed, resulting in 25,984,585 reads and 662 bacterial ASVs retained after all filtering steps [see additional file 1, tables S4 and S5].

Bacterial diversity analyses

Three alpha diversity indexes (Observed, Chao1, Shannon) were calculated in every sample [see additional file 1, table S6]. Statistical comparisons for alpha diversity are shown in additional file 3. Comparisons between matrices (Water and Fish) showed significant differences for the Observed and Chao1 indexes. No differences in alpha diversity were highlighted between males and females. Concerning the different tissues, alpha diversity was significantly highest in skin, followed by the gill and intestine microbiome. Mean Observed index (± std) was 234 ± 47, 217 ± 66 and 66 ± 32 in skin, skin and intestine microbiota, respectively.

Exposure to chemical treatments significantly affected alpha diversity in water, gills and skin but had no effect on the intestine (Fig. 1; additional file 3). Shannon diversity was affected by treatment in water samples, with significantly increased diversity in F2 and Tbz relative to the control treatment [see additional file 3]. Alpha diversity in gill samples (Fig. 1) was influenced by treatment across all three indexes. Gill exposed to F2 had increased Observed and Chao1 values compared to control fish. Gill exposed to F1 had decreased Shannon index values compared to the control and to F2 fish. Skin exposed to F1, F2 and Tbz showed an increase in the Shannon index value compared to the controls (Fig. 1).

Beta diversity and dispersion were next assessed and compared among matrices, tissues and treatment conditions [see additional files 4 and 5]. Beta diversity between matrices was significantly different (fish vs water; $p = 0.002$), and water samples were grouped together, separately from fish samples, on the Bray-Curtis PCoA [see additional file 2, Figure S2A]. Fish sex did not explain variations in beta diversity (male vs female; $p = 0.997$). Tissue type (gill, skin or intestine) accounted for 53.2% of the variance in beta diversity, and samples from each tissue were grouped together, separately from each other, on the Bray-Curtis PCoA [see additional file 2, Figure S2B].

Chemical treatment significantly affected the bacterial beta diversity [see additional file 4]. Water samples were grouped according to treatment condition on the Bray-Curtis PCoA [see additional file 2, Figure S3]. Exposure to fluoride or tebuconazole significantly affected the beta diversity in the gills, with the treatment accounting for 29.5% of variance (PERMANOVA; $p = 0.001$). Pairwise comparisons showed significant differences among all treatment pairs in gills, except between the control and F1. Gill samples from each treatment were grouped together on the Bray-Curtis PCoA (Fig. 2A). In skin samples, beta diversity was also affected by chemical treatment, which explained 20.9% of variance (PERMANOVA; $p = 0.001$). In skin, the control differed significantly from F1, F2 and Tbz, but no differences were detected

among exposed groups (Fig. 2B). Skin samples from each treatment were grouped together on the Bray-Curtis PCoA (Fig. 2B). Concerning intestine samples, although PERMANOVA indicated an overall treatment effect, accounting for 12.1% of the variance ($p = 0.016$), pairwise comparisons showed no significant differences among all treatment pairs (Fig. 2C).

Bacterial taxonomic composition

Bacterial community compositions were represented by the same major phyla among water, gill, skin and intestine samples, but relative abundance differed depending on the tissue type and treatment (Fig. 3). The three dominant phyla in water samples were Bacteroidota (59.5 ± 12.0%), Pseudomonadota (36.0 ± 11.1%) and Bacillota (1.4 ± 1.4%). Gill-associated bacterial communities were mainly represented by Pseudomonadota (37.2 ± 21.1%), Chlamydiota (34.4 ± 23.2%) and Bacteroidota (23.9 ± 19.1%). Skin-associated microbiome was dominated by Pseudomonadota (52.7 ± 14.8%), Bacteroidota (34.1 ± 17.1%) and Bacillota (6.85 ± 13.5%). Intestine microbial communities were mainly composed of Pseudomonadota (64.8 ± 20.8%), Bacillota (23.9 ± 12.0%) and Bacteroidota (9.2 ± 24.5%). Venn diagrams showed that 20% of ASVs were common to all three tissues, and that gill and skin samples shared the largest proportion of ASVs (60%) [see additional file 2, Figure S4].

The Bacillota/Bacteroidota ratio was examined in intestinal samples. It averaged (± std) 253 (± 166) in controls, 370 (± 349) in F1, 45 (± 40) in F2 and 33 (± 40) in Tbz. Treatment had a significant effect on this ratio (Kruskal-Wallis, $\chi^2 = 13.4$, $df = 3$, $p = 0.0039$) and pairwise tests showed a significantly lower ratio in Tbz compared with the control (Dunn Test with Bonferroni correction, $p = 0.0247$).

Differential abundance analyses

Differential abundance analyses were performed independently at the genus level to identify taxa whose abundances differed between exposed and control trout (Fig. 4). In gills, skin and intestine, 35, 21 and 12 genera, respectively, were significantly differentially abundant in at least one exposure treatment compared to the control.

In gills, several abundances shift relative to the control were observed among all treatment conditions: *AAP99*, *Rhizorhapis*, *Polyangium*, *Microbacterium*, *Candidatus Berkiella*, *Shingobium*, *Deefgea* and *Phenylobacterium* (Fig. 4A). Among differentially abundant genera, some potential fish pathogens were enriched in gills following chemical exposure: *Candidatus Piscichlamydia* exhibited a $\log_2$ fold change of 2.1 in F1-exposed trout, *Flavobacterium* of 3.9 and *Aeromonas* of 2.9 in Tbz-exposed trout, each relative to the control (Fig. 4A). A potential human pathogen, *Candidatus Berkiella*, was also increased in gills among all treatment conditions with a $\log_2$ fold change of 4.4 in F1, of 6.6 in F2 and 7.6 in Tbz-exposed fish, each relative to the control (Fig. 4A). A significant increase in the genus *Acidovorax* was also reported following exposure to F2 in gills (Fig. 4A). Relative abundances of *Candidatus Piscichlamydia*, *Flavobacterium* and *Acidovorax* in each gill sample are represented in [see additional file 2, Figure S5].

Microbial communities associated with skin tissue were significantly depleted in *Sphaerotilus* and enriched in *Methylorubrum* and *Phenylobacterium* among all treatment conditions (Fig. 4B). As described in the gill samples, a similar, even though not significant, increase in *Acidovorax* relative abundance was reported following exposure to F2 in the skin-associated microbiome [see additional file 2, Figure S5]. In the intestine microbiome, four of the twelve differentially abundant genera were enriched across all three treatment conditions: *SH-PL-14*, *Candidatus Berkiella*, *Rhizobium* and *Aeromonas* (Fig. 4C). As in the gill microbiome, an enrichment of potential pathogens was highlighted in intestine following chemical exposure: *Flavobacterium* was significantly enriched in Tbz-exposed fish with a $\log_2$ foldchange of 9.3 and *Candidatus Berkiella* was significantly enriched among all treatment conditions with a $\log_2$ foldchange of 20.3 in F1, of 24.0 in F2 and 22.3 in Tbz-exposed fish, each relative to the control (Fig. 4C).

Microbial co-occurrence networks

Co-occurrence networks were inferred using SPIEC-EASI to explore the effects of fluoride exposure (F1 and F2) on gill, skin and intestine microbial interconnections and community structure (Fig. 5; and see additional file 2 Figure S6). Network characteristics were identified and are presented in Table 1. In gills, microbial networks were similar in size across treatments with 305, 268 and 323 nodes and 14, 12 and 13 modules for the control, F1 and F2 treatment conditions, respectively. In gills, fluoride exposure reduced microbial interconnections, decreasing from 897 in the control, to 548 in F1, and showing an intermediate value for F2 (764). Mean node degree followed the same pattern (control: 5.88, F1: 4.09, F2: 4.73), indicating that this reduction reflects fewer connections per node rather than differences in node counts. Modularity values were high among treatments, reflecting that most of the connections occurred within each module, rather than between them. Modularity increased from 0.48 in the control to 0.57 in F1 and 0.53 in F2, highlighting stronger compartmentalisation of microbial networks in gills after fluoride exposure, particularly at the lowest concentration. The bacterial networks associated with skin samples were also similar in size among the control, F1 and F2 treatments with 323, 395 and 386 nodes, and 13, 14 and 14 modules, respectively. While a decrease in microbial interconnections was observed in gills following fluoride exposure, the exact opposite pattern was highlighted in skin microbial communities. Edge count increased from 764 in the control to 1776 in F1 and 1372 in F2 and mean node degree rose accordingly, from 4.73 to 9.00 and 7.11, respectively. Compartmentalisation of networks decreased in fluoride-exposed fish, with modularity dropping from 0.53 in the control to 0.37 in F1 and 0.43 in F2. In intestine samples, node counts were comparable across treatments (control: 127, F1: 162, F2: 143). In the same manner as observed in skin microbial communities, an increase in bacterial interconnections was observed in the intestine following exposure to F1. The module count decreased from 33 (control) to 11 (F1), the edge count increased from 100 (control) to 237 (F1), the mean node degree increased from 1.58 (control) to 2.93 (F1) and the modularity dropped from 0.90 (control) to 0.71 (F1). Intestinal microbial networks in F2-exposed fish showed similar metrics as those observed in control fish. Across tissues, fluoride exposure induced opposite responses in bacterial network structure, with reduced interconnections in gills and increased interconnections in skin and intestine. Despite these contrasting patterns, the strongest network alterations were observed following exposure to the lowest fluoride

concentration (F1), whereas F2 displayed intermediate effects, highlighting that the effects differed depending on the fluoride exposure level.

Table 1
Network characteristics for the microbial co-occurrence networks shown in Fig. 5. Calculations of these properties were performed using igraph functions, as described in the Methods section.

	Gill			Skin			Intestine		
	Control	**F1**	**F2**	**Control**	**F1**	**F2**	**Control**	**F1**	**F2**
No. of samples	12	12	12	11	12	12	11	10	11
No. of nodes	305	268	323	323	395	386	127	162	143
No. of edges	897	548	764	764	1776	1372	100	237	115
No. of modules	14	12	13	13	14	14	33	11	37
Modularity	0.48	0.57	0.53	0.53	0.37	0.43	0.90	0.71	0.90
Mean node degree	5.88	4.09	4.73	4.73	9.00	7.11	1.58	2.93	1.61
Clustering coefficient	0.09	0.07	0.07	0.07	0.11	0.09	0.04	0.09	0.01
Mean path length	3.65	4.46	4.14	4.14	3.12	3.42	4.23	6.55	7.48
Density	0.02	0.02	0.01	0.01	0.02	0.02	0.01	0.02	0.01

Taxonomical composition of each module at the class level was explored for gill, skin and intestine samples among treatments [see additional file 2, Figure S6]. In gills, 21, 17, and 18 taxonomical classes structured the bacterial networks in the control, F1 and F2 treatments, respectively. The number of classes per module was not affected by fluoride exposure. Bacteroidia, Gammaproteobacteria, Actinobacteria and Alphaproteobacteria were the dominant classes structuring the gill bacterial networks across treatments. Chlamydiia appeared in only two modules in the control (modules 7 and 9) but was present in five modules in the F1 treatment (modules 1, 4, 5, 10 and 11), suggesting a stronger structuring role of this taxon following fluoride exposure. In skin, 21, 23 and 24 taxonomical classes structured the bacterial network in the control, F1 and F2 bacterial networks, respectively. Skin bacterial networks were dominated by the same classes as gill microbiomes. Fluoride exposure had little to no impact on the taxonomical composition of the modules structuring the co-occurrence networks. In intestine samples, 7 taxonomical classes were represented in bacterial networks in controls, 12 in F1 and 8 in F2. Alphaproteobacteria, Bacilli and Gammaproteobacteria were the most structuring bacterial classes.

Functional predictions

Functional predictions were generated from metabarcoding data using PICRUSt2, and MetaCyc function pathways were compared among exposure treatments for each tissue using DESeq2 [see additional file

6]. In gills, 32 functional pathways were predicted to be differentially expressed following chemical exposure. Most predicted alterations were associated with Tbz, with 14 disrupted pathways, followed by F1 (10 pathways) and F2 (8 pathways). Compared to control fish, carbohydrate metabolism was the most affected functional category following exposure to F1, vitamin biosynthesis following F2 exposure and aromatic compound metabolism following exposure to Tbz [see additional file 2, Figure S7]. Among differentially expressed pathways in gills, PWY0-1338 (polymyxin resistance) and PWY-6992 (1,5-anhydrofructose degradation), involved in antibiotic resistance, were overexpressed in F2-exposed fish [see additional file 6]. In skin microbiomes, 38 pathways were predicted to be differentially expressed following chemical exposure. In contrast to gills, F2 exposure induced the highest number of predicted disruptions with 20 differentially expressed pathways, followed by F1 (13) and Tbz (5). Exposure to fluoride (F1 and F2) mainly disrupted pathways linked to aromatic compounds metabolism, while Tbz exposure affected carbohydrates and cofactors metabolism [see additional file 2, Figure S7]. Additionally, the predicted pathway PWY-6470 (peptidoglycan biosynthesis V β-lactam resistant) was increased following exposure to both fluoride treatments in skin microbiomes [see additional file 6]. In intestinal microbiomes, 36 pathways were predicted to be differentially expressed following chemical exposure. It concerned 15 pathways in the Tbz treatment group, 11 for F1 and 12 for F2. In the intestine, the distribution of disrupted functional categories appeared more homogeneous compared to gills and skin, with most alterations involving vitamins biosynthesis, C1 compounds, carbohydrates and lipid metabolisms [see additional file 2, Figure S7]. In the intestine, two pathways involved in the steroid metabolism, i.e. potentially involved in hormonal regulation, were differentially expressed following chemical exposure: the predicted pathway PWY-6944 (androstenedione degradation) was increased in F1- and F2-exposed fish and the pathway PWY-6948 (sitosterol degradation to androstenedione) was inhibited after Tbz exposure relative to the control [see additional file 6].

Discussion

Fluoride-induced microbiome disruptions

Rainbow trout chronically exposed to fluoride at 6.8 or 24.7 mg/L exhibited a microbiome shift compared to unexposed fish. Depending on the tissue considered, alpha and beta diversity diverged following exposure; the relative abundances of several taxa, including potential pathogens, were modified and microbial networks and connections were affected. Interestingly, the two tested fluoride concentrations exhibited distinct microbial responses. In gills, alpha diversity was significantly higher in the F2 treatment than in F1 across all indexes, and beta diversity also differed between the two concentrations. Although fluoride-induced alterations of microbial co-occurrence networks were highlighted for both concentrations in gills, skin and intestine, these effects were more pronounced at the lower concentration.

Fluoride is known to exhibit antibacterial and antifungal properties through inferences with the energetic and glycolytic metabolism pathways, as well as by affecting enzyme activity and pH homeostasis of the intracellular environment (93–95). Fluoride-induced buffering of local physicochemical conditions may

create different microbial microenvironments that could lead to selective pressures on microbial taxa and ultimately reorganise the communities (96). Substantial research reported fluoride impacts on the gut microbiome, mainly in humans and rodents (reviewed by Yasin, Zohooriet al.,, 2025 (97)). In the gut microbiome of humans and rodents, fluoride exposure has been linked to shifts in major phyla, such as Bacillota, Bacteroidota and Pseudomonadota, as well as changes in microbial diversity (98, 99). These effects appeared to be strongly dependent on exposure levels, with low concentrations (< 2 mg/L) sometimes promoting the growth of beneficial bacteria such as *Bifidobacterium* and *Lactobacillus*, whereas higher concentrations (> 10 mg/L) can lead to dysbiosis and functional impairment (97).

Only two studies considered the impacts of fluoride on the fish gut microbiome (46, 47), and none have investigated the effects on microbial communities associated with other tissues, such as skin or gill. Microbial community changes were reported in the gut of zebrafish chronically exposed to 80 mg F^-/L for 90 days: both alpha and beta diversity were affected, and the authors observed increases of Pseudomonadota and decreases of Bacteroidota and Planctomycetota (47). Likewise, common carp exposed to 80 mg F^-/L had a lower gut microbial diversity, an increased abundance of Fusobacteria and Bacillota, and a loss of Actinobacteria (46). Both studies linked the gut dysbiosis following fluoride exposure to a loss of integrity of the epithelial barrier: Fluoride induced atrophy and swelling of intestinal villi, destruction of the lamina propria and disrupted expression of tight junction proteins (46, 47).

Differences among these studies and the present work may stem from several factors: First, microbial responses may by dependant on the fish species considered. Second, the type of gut microbiome analysed differed: In this study, the autochthonous, i.e., resident microbiome, was targeted by sampling the mid gut with almost no residual content. On the contrary, Yu, Zhanget al.,, 2021 (46) and Zhang, Chenet al.,, 2022 (47) sampled faeces, which reflects the allochthonous, i.e., transient microbiome, both having their own distinct properties (100). Finally, exposure concentrations also differed, which may account for differences in microbial responses: In the present study, rainbow trout were exposed to 6.8 or 24.7 mg F^-/L, compared to 80 mg F^-/L in previous fish studies. A study performed on mice exposed to 4 mg F^-/L *via* drinking water showed that most of the fluoride was absorbed in the upper gastrointestinal tract (101). Therefore, higher exposure levels (e.g., 80 mg/L) could modify its toxicokinetics and result in enhanced effects along the intestinal tract.

Tebuconazole-induced microbiome disruptions

Tebuconazole is a triazole fungicide, inhibiting an enzyme involved in the synthesis of ergosterol, a key compound of the fungal cell wall (102). By impairing fungal growth and survival, tebuconazole is also expected to affect bacterial communities. Indeed, pollutant effects on bacterial microbiomes are often indirect and mediated through altered microbial interactions (103). In this study, results showed that tebuconazole exposure was associated with increased Alpha diversity (Shannon index) in skin samples and disrupted beta diversity in gill and skin tissues compared to the control. Exposure of zebrafish to 1.2 mg/L of tebuconazole for 21 days also affected the gut beta diversity and taxonomical composition, although the specific taxonomic responses differed, with increased abundances of Pseudomonadota,

Bacillota and Bacteroidota and a decrease of Fusobacteria (104). In an integrative study on the Japanese medaka (*Oryzias latipes*), exposure to 1 mg/L tebuconazole for 60 days increased the gut alpha diversity and altered the taxonomical composition: While beneficial taxa such as *Lactobacillus* or *Cetobacterium* decreased, the abundance of opportunistic and pathogenic bacteria such as *Aeromonas* and *Flavobacterium* increased (58). Authors also highlighted that gut dysbiosis following tebuconazole exposure was associated with alterations in host hepatic metabolism and immune system, suggesting a contribution of microbial imbalance to hepatic dysfunctions *via* the gut-liver axis (58).

In the present study, alterations of the taxonomical composition led to a decreased Bacillota/ Bacteroidota ratio in the gut of Tbz-exposed trout compared to controls. Alteration of this ratio could indicate a dysbiosis, as both phyla are responsible for specific functions within the intestinal microbiome (105–107). Bacillota are involved in fibre fermentation and production of short-chain fatty acids (SCFAs) such as butyrate, acetate or propionate, which take part in the regulation of the gut-brain axis (105, 108). Bacteroidota are involved in the degradation of polysaccharides and fatty acids, and their lipopolysaccharides (LPS) are strong stimulators of innate immunity, therefore impacting immunomodulation and inflammation (105, 108). The Bacillota/ Bacteroidota ratio broadly reflects a balance between energy yield and SFCA production (Bacillota) and polysaccharides degradation coupled with immune signalling (Bacteroidota), suggesting that Tbz-exposed trout may experience a disruption if this equilibrium.

Tissue-specific effects of exposure on microbiomes

Although fluoride or tebuconazole exposure induced changes in bacterial diversity, taxonomical composition and network structures, the nature and magnitude of these effects differed among gills, skin and intestine. While chemical exposure did not affect bacterial alpha nor beta diversity in intestine samples compared to the controls, significant effects were observed in gill and skin microbiomes. Previous studies highlighted this tissue-specific pattern, describing the gut microbiome as more resilient to environmental changes. This resilience could be linked to the fact that gut microbial communities are not directly exposed to the exposure medium, i.e., the surrounding water, and are mainly shaped by species and host factors, more than by environmental conditions (5, 17). In contrast, skin and gill microbiomes showed significant differences in diversity following fluoride and tebuconazole exposure compared to unexposed fish. In fish, the skin microbiome has been described as a sensitive bioindicator of environmental status, responding to physicochemical changes in water (5). For instance, bacterial shifts have been described in the skin microbiome of *Gobio occitaniae* along a water eutrophication gradient, with limited influence of host-specific factors (9). Urbanisation was also reported as a major structuring factor of skin microbiome across different fish species, whereas gut communities appeared less vulnerable to anthropogenic pressures (109). Consistent with these observations, water exposure of rainbow trout to glyphosate had no impact on gut microbial diversity, but significantly altered the gill microbiome, supporting the tissue-specific pattern observed in this study (28).

Although both gill and skin microbiomes responded to fluoride and tebuconazole exposure, their responses were divergent. In gills, exposure to fluoride was associated with a decrease in the Shannon

index, a loss of microbial network connectivity and an increase in compartmentalization. In contrast, the skin microbiome exhibited an increased Shannon diversity across all exposure treatments and showed an opposite network pattern with enhanced microbial interconnections and reduced compartmentalization compared to controls. Comparable results were reported in *Cyprinus carpio* following a 30-min immersion in povidone-iodine (1%), a disinfectant commonly used to prevent and treat bacterial diseases in fish: Gill microbiome showed a decrease in alpha diversity at 3- and 7-day post-exposure, whereas skin diversity tended to increase (110).

Chemical exposure promoted pathogenic bacteria

Trout exposed to the F1 treatment or to tebuconazole exhibited significant increases in the relative abundances of several potential pathogenic bacteria. These increases appeared after an increase of mortality by 2 to 5% of trout in both treatments in the days prior to sampling, suggesting a potential link between microbiome alterations, abundance of pathogenic bacteria and host susceptibility to bacterial diseases. *Candidatus Piscichlamydia* was overrepresented, and the Chlamydiia class had a stronger structuring role in the microbial networks in the gills of F1-exposed fish compared to the control. *C. Piscichlamydia* has already been reported in the trout gills microbiome (28). The intracellular Chlamydia-like bacterium, *C. Piscichlamydia salmonis*, is a causative agent of epitheliocystis, a disease characterized by cyst formation in gill epithelia, leading to impaired respiration and death (111, 112).

Exposure to tebuconazole led to an increase in *Flavobacterium* in both gill and intestine samples compared to controls. While *Flavobacterium* is regularly found in trout microbiomes, its increased abundance following chemical exposure may lead to adverse effects on the host (28). Within this genus, *F. psychrophilum* and *F. columnare* are major threats to aquaculture as they are responsible for the rainbow trout fry syndrome and for the bacterial coldwater disease (113, 114). Similar enrichments of *Flavobacterium* were observed in trout gills following exposure to other environmental contaminants, such as TiO_2 nanoparticles (28 days, 210 µg/L) (115).

In addition, an increase in the opportunistic pathogen *Aeromonas* was also reported in gill and gut microbiota following exposure to fluoride or tebuconazole. *Aeromonas* has been reported to be part of the trout's intestinal core microbiome (114). Nevertheless, increased abundance of some species, including *A. salmonicida*, *A. hydrophila*, *A. veronii*, *A. bestiarum*, *A. caviae*, or *A. sobria*, has been associated with severe pathological outcomes in rainbow trout, such as behavioural alterations, histopathological lesions, septicaemia and furunculosis (116–118). Altogether, these findings are consistent with the hypothesis that disturbances of the environment, e.g., chemical exposure, disrupt the microbial community structure, leading to dysbiosis and the opening of ecological niches favourable to pathogenic taxa (119). This could in turn affect the host immune defences and increase disease susceptibility, as suggested in this study by the parallel increase in potential pathogenic taxa and fish mortality, and as previously demonstrated in pollutant-exposed fish challenged with bacterial pathogens (120).

An increased relative abundance of *Candidatus Berkiella* was also observed in gills and gut microbiomes across all treatment conditions compared to the control. This taxon is an intranuclear bacteria of freshwater amoebae, which can be human parasites causing nearly 100% morbidity for some strains (121, 122). Recently, *Candidatus Berkiella* have been shown to invade and replicate directly in murine and human cell lines, leading authors to suggest that it may represent an early stage in the evolution of a human pathogen (123). As *Candidatus Berkiella* was detected here in rainbow trout, a widely consumed fish species, these findings raise questions concerning possible trophic transfer and potential implications for human health.

Exposure may favour the selection of antibiotic-resistant bacteria

In addition to being opportunistic pathogens, *Aeromonas* spp. can produce extended-spectrum β-lactamases (ESBL), enzymes capable of degrading β-lactam antibiotics (124, 125). An emergence of multidrug-resistant (MDR) *Aeromonas* spp. strains in freshwater environments has also recently been described (125). These strains are a reservoir of antibiotic resistance genes (ARGs) that can be transferred through conjugation, even to phylogenetically distant taxa (125). The increase in *Aeromonas* abundance in the trout microbiomes following exposure to fluoride or tebuconazole could therefore influence ARG dynamics and act as a co-selector of MDR bacteria. Similar results were observed in tebuconazole-contaminated soil ecosystems (0 to 10 mg/L) with increases in the frequency of plasmid conjugative transfer, promoting horizontal transfer of ARGs (126). Authors linked these increases in transfer to the increased abundance of donor bacteria and increased bacterial membrane permeability in donor and recipient bacteria following tebuconazole exposure.

In the present study, an increased abundance of the genus *Acidovorax* was observed in skin in the F2 treatment, and the same pattern, even though not significant, was observed in gill samples compared to the control. This genus has been reported to be enriched in polluted environments, and to be particularly active in the production of quorum-sensing (QS) signals, favouring the communication among bacteria (124, 127). *Acidovorax* spp. are well-known vectors of ARGs, and their QS-mediated signalling, which enhances inter-bacterial interactions and conjugative processes, may facilitate horizontal gene transfer (124, 127). Consequently, their increased abundance following fluoride exposure could enhance ARGs' dissemination within trout microbiomes. Functional prediction pathways also highlighted the potential role of fluoride as a co-selector of ARGs in trout microbiomes. Pathways responsible for polymyxin resistance (PWY0-1338), 1,5-anhydrofructose degradation (PWY-6992) and biosynthesis of β-lactam-resistant peptidoglycan (PWY-6470) were overexpressed following fluoride exposure. Fluoride has been reported to increase reactive oxygen species (ROS), potentially inducing oxidative stress in tissues (45, 128). Such ROS production has been suggested as one of the mechanisms by which pollutant exposure influences horizontal transfer of ARGs within bacterial communities (129). These results, based on functional predictions using 16S rRNA gene metabarcoding data, should be confirmed by metatranscriptomic studies that truly reflect the activity of microorganisms.

From pollutant-induced dysbiosis to endocrine disruption

In this study, the predicted pathway for androstenedione degradation (PWY-6944), a steroid compound, was strongly overexpressed in the gut microbiome in the F1 and F2 treatments compared to the control. Additionally, the predicted pathway for sitosterol degradation to androstenedione (PWY-6948) was inhibited in the gut after Tbz exposure. Fluoride, but also tebuconazole, have been reported as endocrine disruptors in fish, affecting the reproductive and thyroid hormone (TH) systems. In zebrafish, chronic fluoride exposure (0 to 40 mg/L; 20 to 60 days) altered the reproductive hormone levels (LH, FSH, testosterone, estradiol) and gonadal structure (128, 130). It also induced thyroid disruption with changes in TH concentrations and histopathological alterations of thyroid follicles (0 to 80 mg/L, 45 to 90 days) (44, 131). Tebuconazole affects the endocrine axis in a similar manner. Early-life exposure of zebrafish to 0.5 mg/L (0 to 60 dpf) unbalanced the sex ratio and the levels of steroid hormones via aromatase inhibition (56), whereas adult exposure decreased egg production, fertilization success (0 to 1.6 mg/L; 4 months) and disrupted thyroid-related gene expression and TH levels (2 mg/L; 5 days) (132, 133). The observed effects of fluoride or tebuconazole exposure on the trout microbiomes could therefore reflect interactions with endocrine pathways, as both compounds have been reported to exert an endocrine-disrupting activity in fish. These interactions could be two-dimensional: pollutants may disrupt hormonal homeostasis and thereby affect microbial communities, while microbiota dysbiosis may feedback on hormone regulation by affecting (i) bacterial metabolism of circulating steroids which modifies their activity and bioavailability, and (ii) deconjugation and recycling of TH in the gut (134, 135). To clarify these interactions, integrative studies combining microbiomes and hormonal analyses are needed. Finally, while the role of the gut microbiota in hormonal homeostasis is increasingly understood, the roles of the gill and skin microbiota remain unexplored and would need further investigations.

Conclusions

Rainbow trout chronically exposed to fluoride (6.8 and 24.7 mg/L) or to tebuconazole (51.7 µg/L) show shifts in their microbial communities associated with gills, skin and intestine. Exposure to chemical treatments significantly affected bacterial alpha diversity in gills and skin, but had no effect on the intestine, while beta diversity was affected across all three tissues. Microbial co-occurrence networks indicated a loss of interactions following fluoride exposure in the gills, while the opposite, i.e., increased interactions, were observed in the skin and intestine tissues. Exposure also affected the taxonomic composition in the three considered tissues. Genera responsible for fish diseases such as *Candidatus Piscichlamydia*, *Flavobacterium* and *Aeromonas* were increased in gills and intestine following fluoride or tebuconazole exposure. The present study also highlighted an increase in *Candidatus Berkiella*, a potential human pathogen, raising the question of trophic transfer and the implications for human health. We also observed increased abundances of *Acidovorax*, a genus known to carry and transfer antibiotic resistance genes. Finally, predicted functions showed increased expression of pathways responsible for antibiotic resistance following chemical exposure, suggesting a potential co-selection of antibiotic-resistant taxa under chemical pressure. To gain a better understanding of the effects of

chronic fluoride and tebuconazole exposure on the holobiont, it would be valuable to consider bioindicators linked to the host health. As fluoride and tebuconazole exposure favoured pathogenic bacteria, it would be relevant to consider parameters linked to the host immune status. In parallel, indicators of hormonal homeostasis should also be considered, given the described endocrine-disrupting activities of both fluoride and tebuconazole. Moreover, further studies should focus on the functions of microbial communities associated with the different trout tissues and their responses to fluoride and tebuconazole exposure.

Declarations

Ethics approval and consent to participate

European guidelines and recommendations on the protection of animals used for scientific purposes (European Union Directive 2010/63) were strictly followed throughout the entire experiment. Experimental procedures were evaluated and approved by the French Ministry of Higher Education and Research and an animal ethics committee (APAFIS # 39732-2022112416434185 v7). Fish were euthanized by a swift transection of the brainstem, posterior to the head, at the level of the spinal canal, inducing immediate loss of consciousness followed by death. During the experiment, fish showing wounds or severe lesions were submitted to compassionate euthanasia.

Consent for publication

Not applicable

Competing interests

The authors declare that they have no competing interests.

Funding

This work was funded by the French National Research Program for Environmental and Occupational Health of ANSES (ANSES-22-EST-050).

Author Contribution

MS: conceptualization, methodology, formal analysis, investigation, writing (original draft). PP: conceptualization, methodology, writing (review & editing). MD: conceptualization, methodology, writing (review & editing). TB: conceptualization, writing (review & editing). PAG: methodology, investigation, writing (review & editing). JC: conceptualization, methodology, writing (review & editing), supervision,

project administration. LB: conceptualization, methodology, writing (review & editing), supervision, project administration, funding acquisition.

Acknowledgement

Part of the experiments (metabarcoding analysis including library preparation, sequencing and raw data analysis) were performed at the PGTB (https://pgtb.fr/), with the help of Emilie Chancerel and Préscillia Alves-Gomes.

Data Availability

Raw sequencing data are available in the NCBI Sequence Read Archive under BioProject accession number PRJNA1438469.

References

1. Berg G, Rybakova D, Fischer D, Cernava T, Verges MC, Charles T, Chen X, Cocolin L, Eversole K, Corral GH, Kazou M, Kinkel L, Lange L, Lima N, Loy A, Macklin JA, Maguin E, Mauchline T, McClure R, Mitter B, Ryan M, Sarand I, Smidt H, Schelkle B, Roume H, Kiran GS, Selvin J, Souza RSC, van Overbeek L, Singh BK, Wagner M, Walsh A, Sessitsch A, Schloter M. Microbiome definition re-visited: old concepts and new challenges. Microbiome. 2020;8(1):103. 10.1186/s40168-020-00875-0.
2. Llewellyn MS, Boutin S, Hoseinifar SH, Derome N. Teleost microbiomes: the state of the art in their characterization, manipulation and importance in aquaculture and fisheries. Front Microbiol. 2014;5:207. 10.3389/fmicb.2014.00207.
3. Hou K, Wu ZX, Chen XY, Wang JQ, Zhang D, Xiao C, Zhu D, Koya JB, Wei L, Li J, Chen ZS. Microbiota in health and diseases. Signal Transduct Target Ther. 2022;7(1):135. 10.1038/s41392-022-00974-4.
4. Ruiz A, Sanahuja I, Torrecillas S, Gisbert E. Anatomical site and environmental exposure differentially shape the microbiota across mucosal tissues in rainbow trout (*Oncorhynchus mykiss*). Sci Rep. 2025;15(1):25653. 10.1038/s41598-025-11426-8.
5. Sylvain FE, Holland A, Bouslama S, Audet-Gilbert E, Lavoie C, Val AL, Derome N. Fish skin and gut microbiomes show contrasting signatures of host species and habitat. Appl Environ Microbiol. 2020;86(16). 10.1128/AEM.00789-20.
6. Sylvain FE, Cheaib B, Llewellyn M, Gabriel Correia T, Barros Fagundes D, Luis Val A, Derome N. pH drop impacts differentially skin and gut microbiota of the Amazonian fish tambaqui (*Colossoma macropomum*). Sci Rep. 2016;6(1):32032. 10.1038/srep32032.
7. Liu J, Jin S, Zheng Y, Khan FU, Xu J, Fan H, Wang Y, Hu M. Temperature-driven alterations in skin microbiota and biochemistry parameters of sturgeons. Aquaculture. 2025;601:742275. 10.1016/j.aquaculture.2025.742275.

8. Zhou C, Ding F. Analysis of the alterations in symbiotic microbiota and their correlation with intestinal metabolites in rainbow trout (*Oncorhynchus mykiss*) under heat stress conditions. Anim (Basel). 2025;15(14):2017. 10.3390/ani15142017.
9. Cote J, Jacquin L, Veyssiere C, Manzi S, Etienne R, Perrault A, Cambon MC, Jean S, White J. Changes in fish skin microbiota along gradients of eutrophication in human-altered rivers. FEMS Microbiol Ecol. 2022;98(1). 10.1093/femsec/fiac006.
10. Llewellyn MS, McGinnity P, Dionne M, Letourneau J, Thonier F, Carvalho GR, Creer S, Derome N. The biogeography of the atlantic salmon (*Salmo salar*) gut microbiome. ISME J. 2016;10(5):1280–4. 10.1038/ismej.2015.189.
11. Streb LM, Cholewinska P, Gschwendtner S, Geist J, Rath S, Schloter M. Age matters: exploring differential effects of antimicrobial treatment on gut microbiota of adult and juvenile brown trout (*Salmo trutta*). Anim Microbiome. 2025;7(1):28. 10.1186/s42523-025-00391-2.
12. Lokesh J, Kiron V, Sipkema D, Fernandes JMO, Moum T. Succession of embryonic and the intestinal bacterial communities of Atlantic salmon (*Salmo salar*) reveals stage-specific microbial signatures. Microbiologyopen. 2019;8(4):e00672. 10.1002/mbo3.672.
13. Perez-Pascual D, Perez-Cobas AE, Rigaudeau D, Rochat T, Bernardet JF, Skiba-Cassy S, Marchand Y, Duchaud E, Ghigo JM. Sustainable plant-based diets promote rainbow trout gut microbiota richness and do not alter resistance to bacterial infection. Anim Microbiome. 2021;3(1):47. 10.1186/s42523-021-00107-2.
14. Wilkins LG, Fumagalli L, Wedekind C. Effects of host genetics and environment on egg-associated microbiotas in brown trout (*Salmo trutta*). Mol Ecol. 2016;25(19):4930–45. 10.1111/mec.13798.
15. Navarrete P, Magne F, Araneda C, Fuentes P, Barros L, Opazo R, Espejo R, Romero J. PCR-TTGE analysis of 16S rRNA from rainbow trout (*Oncorhynchus mykiss*) gut microbiota reveals host-specific communities of active bacteria. PLoS ONE. 2012;7(2):e31335. 10.1371/journal.pone.0031335.
16. Liu H, Guo X, Gooneratne R, Lai R, Zeng C, Zhan F, Wang W. The gut microbiome and degradation enzyme activity of wild freshwater fishes influenced by their trophic levels. Sci Rep. 2016;6(1):24340. 10.1038/srep24340.
17. McMurtrie J, Bell AG, Cable J, Temperton B, Tyler CR. The ecology and plasticity of fish skin and gill microbiomes: seeking what matters in health and disease. FEMS Microbiol Rev. 2025;49. 10.1093/femsre/fuaf027.
18. Amillano-Cisneros JM, Fuentes-Valencia MA, Leyva-Morales JB, Davizon YA, Marquez-Pacheco H, Valencia-Castaneda G, Maldonado-Coyac JA, Ontiveros-Garcia LA, Badilla-Medina CN. Prebiotics in global and Mexican fish aquaculture: A review. Anim (Basel). 2023;13(23):3607. 10.3390/ani13233607.
19. Mendez-Martinez Y, Campa-Cordova AI, Luna-Gonzalez A, Editorial. Innovative approaches to modulate fish gut microbiota for disease management in aquaculture. Front Microbiol. 2025;16:1721029. 10.3389/fmicb.2025.1721029.

20. Legrand T, Catalano SR, Wos-Oxley ML, Stephens F, Landos M, Bansemer MS, Stone DAJ, Qin JG, Oxley APA. The inner workings of the outer surface: skin and gill microbiota as indicators of changing gut health in yellowtail kingfish. Front Microbiol. 2017;8:2664. 10.3389/fmicb.2017.02664.
21. Evans DH, Piermarini PM, Choe KP. The multifunctional fish gill: dominant site of gas exchange, osmoregulation, acid-base regulation, and excretion of nitrogenous waste. Physiol Rev. 2005;85(1):97–177. 10.1152/physrev.00050.2003.
22. Reverter M, Tapissier-Bontemps N, Lecchini D, Banaigs B, Sasal P. Biological and ecological roles of external fish mucus: A review. Fishes. 2018;3(4):41. 10.3390/fishes3040041.
23. Gomez JA, Primm TP. A slimy business: the future of fish skin microbiome studies. Microb Ecol. 2021;82(2):275–87. 10.1007/s00248-020-01648-w.
24. Dong B, Moon HB. Toxicological effects of chemical pesticides in fish: Focusing on intestinal injury and gut microbial dysbiosis. Pestic Biochem Physiol. 2025;211:106405. 10.1016/j.pestbp.2025.106405.
25. Evariste L, Barret M, Mottier A, Mouchet F, Gauthier L, Pinelli E. Gut microbiota of aquatic organisms: A key endpoint for ecotoxicological studies. Environ Pollut. 2019;248:989–99. 10.1016/j.envpol.2019.02.101.
26. Duperron S, Halary S, Gallet A, Marie B. Microbiome-aware ecotoxicology of organisms: Relevance, pitfalls, and challenges. Front Public Health. 2020;8:407. 10.3389/fpubh.2020.00407.
27. Guerrero R, Margulis L, Berlanga M. Symbiogenesis: the holobiont as a unit of evolution. Int Microbiol. 2013;16(3):133–43. 10.2436/20.1501.01.188.
28. Bellec L, Le Du-Carre J, Almeras F, Durand L, Cambon-Bonavita MA, Danion M, Morin T. Glyphosate-based herbicide exposure: effects on gill microbiota of rainbow trout (*Oncorhynchus mykiss*) and the aquatic bacterial ecosystem. FEMS Microbiol Ecol. 2022;98(8). 10.1093/femsec/fiac076.
29. Bellec L, Milinkovitch T, Dubillot E, Pante E, Tran D, Lefrancois C. Fish gut and skin microbiota dysbiosis induced by exposure to commercial sunscreen formulations. Aquat Toxicol. 2024;266:106799. 10.1016/j.aquatox.2023.106799.
30. Huang JN, Zhang Y, Xu L, He KX, Wen B, Yang PW, Ding JY, Li JZ, Ma HC, Gao JZ, Chen ZZ. Microplastics: A tissue-specific threat to microbial community and biomarkers of discus fish (*Symphysodon aequifasciatus*). J Hazard Mater. 2022;424(Pt D):127751. 10.1016/j.jhazmat.2021.127751.
31. Yang Y, Yan C, Li A, Qiu J, Yan W, Dang H. Effects of the plastic additive 2,4-di-tert-butylphenol on intestinal microbiota of zebrafish. J Hazard Mater. 2024;469:133987. 10.1016/j.jhazmat.2024.133987.
32. Liu Y, Yao Y, Li H, Qiao F, Wu J, Du ZY, Zhang M. Influence of endogenous and exogenous estrogenic endocrine on intestinal microbiota in zebrafish. PLoS ONE. 2016;11(10):e0163895. 10.1371/journal.pone.0163895.
33. Camargo JA. Fluoride toxicity to aquatic organisms: a review. Chemosphere. 2003;50(3):251–64. 10.1016/s0045-6535(02)00498-8.

34. WHO, Fluorides IPCS. International Programme on Chemical Safety (Environmental Health Criteria 227). Geneva: World Health Organization; 2002.
35. Muthu Prabhu S, Yusuf M, Ahn Y, Park HB, Choi J, Amin MA, Yadav KK, Jeon BH. Fluoride occurrence in environment, regulations, and remediation methods for soil: A comprehensive review. Chemosphere. 2023;324:138334. 10.1016/j.chemosphere.2023.138334.
36. Kitalika AJ, Machunda RL, Komakech HC, Njau KN. Fluoride variations in rivers on the slopes of mount Meru in Tanzania. J Chem. 2018;2018:1–18. 10.1155/2018/7140902.
37. Kim WT, Lee JW, An HE, Cho SH, Jeong S. Efficient fluoride wastewater treatment using eco-friendly synthesized AlOOH. Nanomaterials (Basel). 2023;13(21):2838. 10.3390/nano13212838.
38. Bagastyo AY, Anggrainy AD, Nindita CS, Warmadewanthi. Electrodialytic removal of fluoride and calcium ions to recover phosphate from fertilizer industry wastewater. Sustainable Environ Res. 2017;27(5):230–7. 10.1016/j.serj.2017.06.002.
39. Sellers C. The artificial nature of fluoridated water: between nations, knowledge, and material flows. Osiris. 2004;19(1):182–200. 10.1086/649401.
40. EFSA. Scientific opinion on dietary reference values for fluoride. EFSA J. 2013;11(8):3332. 10.2903/j.efsa.2013.3332.
41. Peckham S, Awofeso N. Water fluoridation: a critical review of the physiological effects of ingested fluoride as a public health intervention. ScientificWorldJournal. 2014;2014:293019. 10.1155/2014/293019.
42. Yadav SS, Kumar R, Khare P, Tripathi M. Oxidative stress biomarkers in the freshwater fish, *Heteropneustes fossilis* (Bloch) exposed to sodium fluoride: antioxidant defense and role of ascorbic acid. Toxicol Int. 2015;22(1):71–6. 10.4103/0971-6580.172261.
43. Chen J, Luo Y, Cao J, Xie L. Fluoride exposure changed the expression of microRNAs in gills of male zebrafish (*Danio rerio*). Aquat Toxicol. 2021;233:105789. 10.1016/j.aquatox.2021.105789.
44. Jianjie C, Wenjuan X, Jinling C, Jie S, Ruhui J, Meiyan L. Fluoride caused thyroid endocrine disruption in male zebrafish (*Danio rerio*). Aquat Toxicol. 2016;171:48–58. 10.1016/j.aquatox.2015.12.010.
45. Wei YL, Lin XC, Liu YY, Lei YQ, Zhuang XD, Zhang HT, Wang XR. Effects of water fluoridation on early embryonic development of zebrafish. Ecotoxicol Environ Saf. 2024;270:115907. 10.1016/j.ecoenv.2023.115907.
46. Yu H, Zhang Y, Zhang P, Shang X, Lu Y, Fu Y, Li Y. Effects of fluorine on intestinal structural integrity and microbiota composition of common carp. Biol Trace Elem Res. 2021;199(9):3489–96. 10.1007/s12011-020-02456-6.
47. Zhang X, Chen J, Wang G, Chen H, Cao J, Xie L, Luo Y. Interactive effects of fluoride and seleno-l-methionine at environmental related concentrations on zebrafish (*Danio rerio*) liver via the gut-liver axis. Fish Shellfish Immunol. 2022;127:690–702. 10.1016/j.fsi.2022.07.006.
48. INERIS. Institut national de l'environnement industriel et des risques, Tébuconazole, Verneuil-en-Halatte. Ineris – 181229 - v3.0, 08/05/2020. 2020.

49. Zubrod JP, Bundschuh M, Arts G, Bruhl CA, Imfeld G, Knabel A, Payraudeau S, Rasmussen JJ, Rohr J, Scharmuller A, Smalling K, Stehle S, Schulz R, Schafer RB. Fungicides: An overlooked pesticide class? Environ Sci Technol. 2019;53(7):3347–65. 10.1021/acs.est.8b04392.
50. Paijens C, Tedoldi D, Frère B, Mailler R, Rocher V, Moilleron R, Bressy A. Biocidal substances in the Seine River: contribution from urban sources in the Paris megacity. Environ Science: Water Res Technol. 2022;8(10):2358–72. 10.1039/d2ew00253a.
51. Chaumet B, Probst JL, Payre-Suc V, Granouillac F, Riboul D, Probst A. Pond mitigation in dissolved and particulate pesticide transfers: Influence of storm events and seasonality (Aurade agricultural catchment, SW-France). J Environ Manage. 2022;320:115911. 10.1016/j.jenvman.2022.115911.
52. Lefrancq M, Jadas-Hecart A, La Jeunesse I, Landry D, Payraudeau S. High frequency monitoring of pesticides in runoff water to improve understanding of their transport and environmental impacts. Sci Total Environ. 2017;587–588:75–86. 10.1016/j.scitotenv.2017.02.022.
53. Li S, Jiang Y, Sun Q, Coffin S, Chen L, Qiao K, Gui W, Zhu G. Tebuconazole induced oxidative stress related hepatotoxicity in adult and larval zebrafish (*Danio rerio*). Chemosphere. 2020;241:125129. 10.1016/j.chemosphere.2019.125129.
54. Sancho E, Villarroel MJ, Fernandez C, Andreu E, Ferrando MD. Short-term exposure to sublethal tebuconazole induces physiological impairment in male zebrafish (*Danio rerio*). Ecotoxicol Environ Saf. 2010;73(3):370–6. 10.1016/j.ecoenv.2009.09.020.
55. Macirella R, Curcio V, Ahmed AIM, Pellegrino D, Brunelli E. Effect of short-term exposure to low concentration of tebuconazole: morphological, histometric and functional modifications in *Danio rerio* liver. Eur Zoological J. 2022;89(1):331–45. 10.1080/24750263.2022.2043469.
56. Qiao K, Liang Z, Wang A, Wu Q, Yang S, Ma Y, Li S, Schiwy S, Jiang J, Zhou S, Ye Q, Hollert H, Gui W. Waterborne tebuconazole exposure induces male-biased sex differentiation in zebrafish (*Danio rerio*) larvae via aromatase inhibition. Environ Sci Technol. 2023;57(44):16764–78. 10.1021/acs.est.3c03181.
57. Huang T, Zhao Y, He J, Cheng H, Martyniuk CJ. Endocrine disruption by azole fungicides in fish: A review of the evidence. Sci Total Environ. 2022;822:153412. 10.1016/j.scitotenv.2022.153412.
58. Jawad M, Xu H, Nasir S, Yin J, Wu C, Wang A, Hong N, Li M. Microbial dysbiosis and hepatic inflammation under combined pesticide exposure: Insights into gut-liver axis disruption in Japanese medaka. J Hazard Mater. 2025;499:140295. 10.1016/j.jhazmat.2025.140295.
59. FAO. The state of world fisheries and aquaculture 2022. Towards blue transformation. Food and Agriculture Organization of the United Nations. 2022. 10.4060/cc0461en
60. Camargo JA, Tarazona JV. Short-term toxicity of fluoride ion (F^-) in soft water to rainbow trout and brown trout. Chemosphere. 1991;22(5–6):605–11. 10.1016/0045-6535(91)90071-k.
61. Angelovic JW, Sigler WF, Neuhold JM. Temperature and fluorosis in rainbow trout. J Water Pollution Control Federation. 1961;33(4):371–81.
62. Er A. Short-term exposure to tebuconazole triggers haematological, histological and biochemical disturbances in rainbow trout (*Oncorhynchus mykiss*). Toxics. 2025;13(8):630.

10.3390/toxics13080630.

63. Handy RD. Intermittent exposure to aquatic pollutants: assessment, toxicity and sublethal responses in fish and invertebrates. Comparative Biochemistry and Physiology Part C: Pharmacology. Toxicol Endocrinol. 1994;107(2):171–84. 10.1016/1367-8280(94)90039-6.
64. Colvin MA, Kowal KR, Hayman NT, Stransky C, VanVoorhis J, Carlson S, Rosen G. Pulsed exposure toxicity testing: Baseline evaluations and considerations using copper and zinc with two marine species. Chemosphere. 2021;277:130323. 10.1016/j.chemosphere.2021.130323.
65. Boxall AB, Fogg LA, Ashauer R, Bowles T, Sinclair CJ, Colyer A, Brain RA. Effects of repeated pulsed herbicide exposures on the growth of aquatic macrophytes. Environ Toxicol Chem. 2013;32(1):193–200. 10.1002/etc.2040.
66. Amachree D, Moody AJ, Handy RD. Comparison of intermittent and continuous exposures to inorganic mercury in the mussel, *Mytilus edulis*: accumulation and sub-lethal physiological effects. Ecotoxicol Environ Saf. 2014;109:133–42. 10.1016/j.ecoenv.2014.07.025.
67. Li H, Zhang W, Yan H, Gao P. Understanding the toxicity risk of antibiotic emissions of aquaculture from the perspective of fluctuations concentration. Environ Pollut. 2024;351:124024. 10.1016/j.envpol.2024.124024.
68. Pannetier P, Baumann L, Braunbeck T, Stoll M, Supiot L, Lannuzel G, Louboutin L, Grippon P, Bellec L, Morin T, Danion M. Chronic exposure to sodium fluoride or to tebuconazole disrupts the thyroid and immune systems during the early life stages of rainbow trout (*Oncorhynchus mykiss*). *Submitted to Aquatic Toxicology, preprint available*. 2026. http://dx.doi.org/10.2139/ssrn.6552359
69. Ricker WE. Computation and interpretation of biological statistics of fish populations. Fish Res Board Can Bull. 1975;191:1–382.
70. Rud YP, Buchatsky L. The rapid diagnostics of sex of salmonids using DNA-markers. Biotechnologia Acta. 2014;7(6):17–22.
71. Klindworth A, Pruesse E, Schweer T, Peplies J, Quast C, Horn M, Glockner FO. Evaluation of general 16S ribosomal RNA gene PCR primers for classical and next-generation sequencing-based diversity studies. Nucleic Acids Res. 2013;41(1):e1. 10.1093/nar/gks808.
72. Escudie F, Auer L, Bernard M, Mariadassou M, Cauquil L, Vidal K, Maman S, Hernandez-Raquet G, Combes S, Pascal G. FROGS: Find, Rapidly, OTUs with Galaxy Solution. Bioinformatics. 2018;34(8):1287–94. 10.1093/bioinformatics/btx791.
73. Rognes T, Flouri T, Nichols B, Quince C, Mahe F. VSEARCH: a versatile open source tool for metagenomics. PeerJ. 2016;4:e2584. 10.7717/peerj.2584.
74. Callahan BJ, McMurdie PJ, Rosen MJ, Han AW, Johnson AJ, Holmes SP. DADA2: High-resolution sample inference from Illumina amplicon data. Nat Methods. 2016;13(7):581–3. 10.1038/nmeth.3869.
75. Bokulich NA, Subramanian S, Faith JJ, Gevers D, Gordon JI, Knight R, Mills DA, Caporaso JG. Quality-filtering vastly improves diversity estimates from Illumina amplicon sequencing. Nat Methods. 2013;10(1):57–9. 10.1038/nmeth.2276.

76. Chen Y, Ye W, Zhang Y, Xu Y. High speed BLASTN: an accelerated MegaBLAST search tool. Nucleic Acids Res. 2015;43(16):7762–8. 10.1093/nar/gkv784.
77. Cole JR, Wang Q, Fish JA, Chai B, McGarrell DM, Sun Y, Brown CT, Porras-Alfaro A, Kuske CR, Tiedje JM. Ribosomal Database Project: data and tools for high throughput rRNA analysis. Nucleic Acids Res. 2014;42(Database issue):D633–42. 10.1093/nar/gkt1244.
78. Yilmaz P, Parfrey LW, Yarza P, Gerken J, Pruesse E, Quast C, Schweer T, Peplies J, Ludwig W, Glockner FO. The SILVA and All-species Living Tree Project (LTP) taxonomic frameworks. Nucleic Acids Res. 2014;42(Database issue):D643–8. 10.1093/nar/gkt1209.
79. Quast C, Pruesse E, Yilmaz P, Gerken J, Schweer T, Yarza P, Peplies J, Glockner FO. The SILVA ribosomal RNA gene database project: improved data processing and web-based tools. Nucleic Acids Res. 2013;41(Database issue):D590–6. 10.1093/nar/gks1219.
80. McKnight DT, Huerlimann R, Bower DS, Schwarzkopf L, Alford RA, Zenger KR. microDecon: A highly accurate read-subtraction tool for the post-sequencing removal of contamination in metabarcoding studies. Environ DNA. 2019;1(1):14–25. 10.1002/edn3.11.
81. McMurdie PJ, Holmes S. phyloseq: an R package for reproducible interactive analysis and graphics of microbiome census data. PLoS ONE. 2013;8(4):e61217. 10.1371/journal.pone.0061217.
82. Paulson JN, Talkuder H, Pop M, Bravo HC. metagenomeSeq: Statistical analysis for sparse high-throughput sequencing. Bioconductor package. 2013;1(0):191.
83. Dixon P. VEGAN, a package of R functions for community ecology. J Veg Sci. 2003;14(6):927–30. 10.1111/j.1654-1103.2003.tb02228.x.
84. Martinez Arbizu P, pairwiseAdonis. Pairwise multilevel comparison using adonis. R package version 0.4. 2020.
85. Love MI, Huber W, Anders S. Moderated estimation of fold change and dispersion for RNA-seq data with DESeq2. Genome Biol. 2014;15(12):550. 10.1186/s13059-014-0550-8.
86. Gao CH, Chen C, Akyol T, Dusa A, Yu G, Cao B, Cai P. ggVennDiagram: Intuitive Venn diagram software extended. Imeta. 2024;3(1):e177. 10.1002/imt2.177.
87. Kurtz ZD, Muller CL, Miraldi ER, Littman DR, Blaser MJ, Bonneau RA. Sparse and compositionally robust inference of microbial ecological networks. PLoS Comput Biol. 2015;11(5):e1004226. 10.1371/journal.pcbi.1004226.
88. Csardi G, Nepusz T. The igraph software. Complex syst. 2006;1695:1–9. https://igraph.org/.
89. Douglas GM, Maffei VJ, Zaneveld JR, Yurgel SN, Brown JR, Taylor CM, Huttenhower C, Langille MGI. PICRUSt2 for prediction of metagenome functions. Nat Biotechnol. 2020;38(6):685–8. 10.1038/s41587-020-0548-6.
90. Barbera P, Kozlov AM, Czech L, Morel B, Darriba D, Flouri T, Stamatakis A. EPA-ng: Massively parallel evolutionary placement of genetic sequences. Syst Biol. 2019;68(2):365–9. 10.1093/sysbio/syy054.
91. Czech L, Barbera P, Stamatakis A. Genesis and Gappa: processing, analyzing and visualizing phylogenetic (placement) data. Bioinformatics. 2020;36(10):3263–5.

10.1093/bioinformatics/btaa070.

92. Ye Y, Doak TG. A parsimony approach to biological pathway reconstruction/inference for genomes and metagenomes. PLoS Comput Biol. 2009;5(8):e1000465. 10.1371/journal.pcbi.1000465.
93. Van Loveren C. Antimicrobial activity of fluoride and its *in vivo* importance: identification of research questions. Caries Res. 2001;35(Suppl 1):65–70. 10.1159/000049114.
94. Han Y. Effects of brief sodium fluoride treatments on the growth of early and mature cariogenic biofilms. Sci Rep. 2021;11(1):18290. 10.1038/s41598-021-97905-0.
95. Johnston NR, Strobel SA. Principles of fluoride toxicity and the cellular response: a review. Arch Toxicol. 2020;94(4):1051–69. 10.1007/s00204-020-02687-5.
96. Lopez-Lopez A, Mira A. Shifts in composition and activity of oral biofilms after fluoride exposure. Microb Ecol. 2020;80(3):729–38. 10.1007/s00248-020-01531-8.
97. Yasin M, Zohoori FV, Kumah EA, Subramanian M, Dean P, Orr CH. Effect of fluoride on gut microbiota: A systematic review. Nutr Rev. 2025;83(7):e1853–80. 10.1093/nutrit/nuae202.
98. Wang J, Yu C, Zhang J, Liu R, Xiao J. Aberrant gut microbiota and fecal metabolites in patients with coal-burning endemic fluorosis in Guizhou, China. Environ Sci Pollut Res Int. 2023;30(27):69913–26. 10.1007/s11356-023-27051-9.
99. Zhou G, Li Q, Hou X, Wu H, Fu X, Wang G, Ma J, Cheng X, Yang Y, Chen R, Li Z, Yu F, Zhu J, Ba Y. Integrated 16S rDNA sequencing and metabolomics to explore the intestinal changes in children and rats with dental fluorosis. Ecotoxicol Environ Saf. 2023;251:114518. 10.1016/j.ecoenv.2023.114518.
100. Tarnecki AM, Burgos FA, Ray CL, Arias CR. Fish intestinal microbiome: diversity and symbiosis unravelled by metagenomics. J Appl Microbiol. 2017;123(1):2–17. 10.1111/jam.13415.
101. Yasuda K, Hsu T, Gallini CA, McLver LJ, Schwager E, Shi A, DuLong CR, Schwager RN, Abu-Ali GS, Franzosa EA, Garrett WS, Huttenhower C, Morgan XC. Fluoride depletes acidogenic taxa in oral but not gut microbial communities in mice. mSystems. 2017;2(4):e00047–17. 10.1128/mSystems.00047-17.
102. Dong B. A comprehensive review on toxicological mechanisms and transformation products of tebuconazole: Insights on pesticide management. Sci Total Environ. 2024;908:168264. 10.1016/j.scitotenv.2023.168264.
103. Meyer C, Jeanbille M, Breuil MC, Bru D, Hofer K, Screpanti C, Philippot L. Soil microbial community fragmentation reveals indirect effects of fungicide exposure mediated by biotic interactions between microorganisms. J Hazard Mater. 2024;470:134231. 10.1016/j.jhazmat.2024.134231.
104. Jiang J, Chen L, Liu X, Wang L, Wu S, Zhao X. Histology and multi-omic profiling reveal the mixture toxicity of tebuconazole and difenoconazole in adult zebrafish. Sci Total Environ. 2021;795:148777. 10.1016/j.scitotenv.2021.148777.
105. Magne F, Gotteland M, Gauthier L, Zazueta A, Pesoa S, Navarrete P, Balamurugan R. The Firmicutes/Bacteroidetes ratio: A relevant marker of gut dysbiosis in obese patients? Nutrients. 2020;12(5):1474. 10.3390/nu12051474.

106. Hu J, Raikhel V, Gopalakrishnan K, Fernandez-Hernandez H, Lambertini L, Manservisi F, Falcioni L, Bua L, Belpoggi F, Chen SLT. Effect of postnatal low-dose exposure to environmental chemicals on the gut microbiome in a rodent model. Microbiome. 2016;4(1):26. 10.1186/s40168-016-0173-2.
107. Tian X, Yu Z, Feng P, Ye Z, Li R, Liu J, Hu J, Kakade A, Liu P, Li X. *Lactobacillus plantarum* TW1-1 alleviates diethylhexylphthalate-induced testicular damage in mice by modulating gut microbiota and decreasing inflammation. Front Cell Infect Microbiol. 2019;9:221. 10.3389/fcimb.2019.00221.
108. Stojanov S, Berlec A, Strukelj B. The influence of probiotics on the Firmicutes/Bacteroidetes ratio in the treatment of obesity and inflammatory bowel disease. Microorganisms. 2020;8(11):1715. 10.3390/microorganisms8111715.
109. Colin Y, Berthe T, Molbert N, Guigon E, Vivant AL, Alliot F, Collin S, Goutte A, Petit F. Urbanization constrains skin bacterial phylogenetic diversity in wild fish populations and correlates with the proliferation of Aeromonads. Microb Ecol. 2021;82(2):523–36. 10.1007/s00248-020-01650-2.
110. Zhang R, Wu GT, Zhu JY, Wang XW, Liu LL, Li HJ, Zhu H. Povidone iodine exposure alters the immune response and microbiota of the gill and skin in koi carp, *Cyprinus carpio*. Aquaculture. 2023;563:738926. 10.1016/j.aquaculture.2022.738926.
111. Draghi A 2nd, Popov VL, Kahl MM, Stanton JB, Brown CC, Tsongalis GJ, West AB, Frasca S. Jr. Characterization of *Candidatus Piscichlamydia salmonis* (order Chlamydiales), a chlamydia-like bacterium associated with epitheliocystis in farmed Atlantic salmon (*Salmo salar*). J Clin Microbiol. 2004;42(11):5286–97. 10.1128/JCM.42.11.5286-5297.2004.
112. Blandford MI, Taylor-Brown A, Schlacher TA, Nowak B, Polkinghorne A. Epitheliocystis in fish: An emerging aquaculture disease with a global impact. Transbound Emerg Dis. 2018;65(6):1436–46. 10.1111/tbed.12908.
113. Boutin S, Bernatchez L, Audet C, Derome N. Antagonistic effect of indigenous skin bacteria of brook charr (*Salvelinus fontinalis*) against *Flavobacterium columnare* and *F. psychrophilum*. Vet Microbiol. 2012;155(2–4):355–61. 10.1016/j.vetmic.2011.09.002.
114. Takeuchi M, Sugahara K. Systematic literature review identifying core genera in the gut microbiome of rainbow trout (*Oncorhynchus mykiss*) and species-level microbial community analysis using long-read amplicon sequencing. Aquaculture Fish Fisheries. 2025;5(2). 10.1002/aff2.70054.
115. Beghin M, Ambroise V, Lambert J, Garigliany MM, Cornet V, Kestemont P. Environmental exposure to single and combined ZnO and TiO(2) nanoparticles: Implications for rainbow trout gill immune functions and microbiota. Chemosphere. 2025;373:144148. 10.1016/j.chemosphere.2025.144148.
116. Gómez de Anda FR, Vega-Sánchez V, Reyes-Rodríguez NE, Martínez-Juárez VM, Ángeles-Hernández JC, Acosta-Rodríguez I, Campos-Montiel RG, Zepeda-Velázquez AP. The nasal epithelium as a route of infection and clinical signs changes, in rainbow trout (*Oncorhynchus mykiss*) fingerlings infected with *Aeromonas spp*. Appl Sci. 2021;11(19):9159. 10.3390/app11199159.
117. Zepeda-Velazquez AP, Vega-Sanchez V, Salgado-Miranda C, Soriano-Vargas E. Histopathological findings in farmed rainbow trout (*Oncorhynchus mykiss*) naturally infected with 3 different *Aeromonas* species. Can J Vet Res. 2015;79(3):250–4.

118. Akram M, Hafeez-ur-Rehman M, Abbas F, Altaf I, Kanwal S, Mobeen N, Khaliq A, Sharif A, Tayyaba M, Talib S, Riaz MN, Zafar S, Hussain I, Khan KJ, Sughra F. Identification, isolation and pathogenicity of *Aeromonas salmonicida* and his-topathology of infected *Oncorhynchus mykiss* in Punjab and northern areas of Pakistan. J Fisheries. 2025;13(1):131204. 10.17017/j.fish.683.
119. Boutin S, Bernatchez L, Audet C, Derome N. Network analysis highlights complex interactions between pathogen, host and commensal microbiota. PLoS ONE. 2013;8(12):e84772. 10.1371/journal.pone.0084772.
120. Mohammed HH, Arias CR. Potassium permanganate elicits a shift of the external fish microbiome and increases host susceptibility to columnaris disease. Vet Res. 2015;46(1):82. 10.1186/s13567-015-0215-y.
121. Scheid P. Free-living amoebae as human parasites and hosts for pathogenic microorganisms. Proceedings. 2018;2(11):692. 10.3390/proceedings2110692
122. Mehari YT, Jason Hayes B, Redding KS, Mariappan PVG, Gunderson JH, Farone AL, Farone MB. Description of '*Candidatus Berkiella aquae*' and '*Candidatus Berkiella cookevillensis*', two intranuclear bacteria of freshwater amoebae. Int J Syst Evol Microbiol. 2016;66(2):536–41. 10.1099/ijsem.0.000750.
123. Chamberlain NB, Mehari YT, Hayes BJ, Roden CM, Kidane DT, Swehla AJ, Lorenzana-DeWitt MA, Farone AL, Gunderson JH, Berk SG, Farone MB. Infection and nuclear interaction in mammalian cells by '*Candidatus Berkiella cookevillensis*', a novel bacterium isolated from amoebae. BMC Microbiol. 2019;19(1):91. 10.1186/s12866-019-1457-z.
124. Malik SS, Loganathachetti DS, Khan MA, Sadaiappan B, Mundra S. Bacterial resistome in different stages of wastewater treatment plant is highly impacted by the abundance of the Pseudomonadota community. Bioresource Technol Rep. 2024;26:101814. 10.1016/j.biteb.2024.101814.
125. Bello-Lopez JM, Cabrero-Martinez OA, Ibanez-Cervantes G, Hernandez-Cortez C, Pelcastre-Rodriguez LI, Gonzalez-Avila LU, Castro-Escarpulli G. Horizontal gene transfer and its association with antibiotic resistance in the genus *Aeromonas spp*. Microorganisms. 2019;7(9):363. 10.3390/microorganisms7090363.
126. Gao Y, Guo Y, Wang L, Guo L, Shi B, Zhu L, Wang J, Kim YM, Wang J. Tebuconazole exacerbates co-occurrence and horizontal transfer of antibiotic resistance genes. Pestic Biochem Physiol. 2024;204:106026. 10.1016/j.pestbp.2024.106026.
127. Huang H, Chen Y, Yang S, Zheng X. CuO and ZnO nanoparticles drive the propagation of antibiotic resistance genes during sludge anaerobic digestion: possible role of stimulated signal transduction. Environ Science: Nano. 2019;6(2):528–39. 10.1039/c8en00370j.
128. Li M, Cao J, Zhao Y, Wu P, Li X, Khodaei F, Han Y, Wang J. Fluoride impairs ovary development by affecting oogenesis and inducing oxidative stress and apoptosis in female zebrafish (*Danio rerio*). Chemosphere. 2020;256:127105. 10.1016/j.chemosphere.2020.127105.
129. Feng G, Huang H, Chen Y. Effects of emerging pollutants on the occurrence and transfer of antibiotic resistance genes: A review. J Hazard Mater. 2021;420:126602. 10.1016/j.jhazmat.2021.126602.

130. Li M, Cao J, Chen J, Song J, Zhou B, Feng C, Wang J. Waterborne fluoride exposure changed the structure and the expressions of steroidogenic-related genes in gonads of adult zebrafish (*Danio rerio*). Chemosphere. 2016;145:365–75. 10.1016/j.chemosphere.2015.11.041.
131. Lu Y, Zhang X, Chen J, Cao J, Feng C, Yun S, Cheng Y, Cheng F. Sex-specific effects of fluoride and lead on thyroid endocrine function in zebrafish (*Danio rerio*). Chem Biol Interact. 2022;367:110151. 10.1016/j.cbi.2022.110151.
132. Yan W, Li G, Lu Q, Hou J, Pan M, Peng M, Peng X, Wan H, Liu X, Wu Q. Molecular mechanisms of tebuconazole affecting the social behavior and reproduction of zebrafish. Int J Environ Res Public Health. 2023;20(5):3928. 10.3390/ijerph20053928.
133. Yu L, Chen M, Liu Y, Gui W, Zhu G. Thyroid endocrine disruption in zebrafish larvae following exposure to hexaconazole and tebuconazole. Aquat Toxicol. 2013;138–139:35–42. 10.1016/j.aquatox.2013.04.001.
134. Fenneman AC, Bruinstroop E, Nieuwdorp M, van der Spek AH, Boelen A. A comprehensive review of thyroid hormone metabolism in the gut and its clinical implications. Thyroid. 2023;33(1):32–44. 10.1089/thy.2022.0491.
135. Ly LK, Rowles JL 3rd, Paul HM, Alves JMP, Yemm C, Wolf PM, Devendran S, Hudson ME, Morris DJ, Erdman JW Jr., Ridlon JM. Bacterial steroid-17,20-desmolase is a taxonomically rare enzymatic pathway that converts prednisone to 1,4-androstanediene-3,11,17-trione, a metabolite that causes proliferation of prostate cancer cells. J Steroid Biochem Mol Biol. 2020;199:105567. 10.1016/j.jsbmb.2019.105567.

Figures

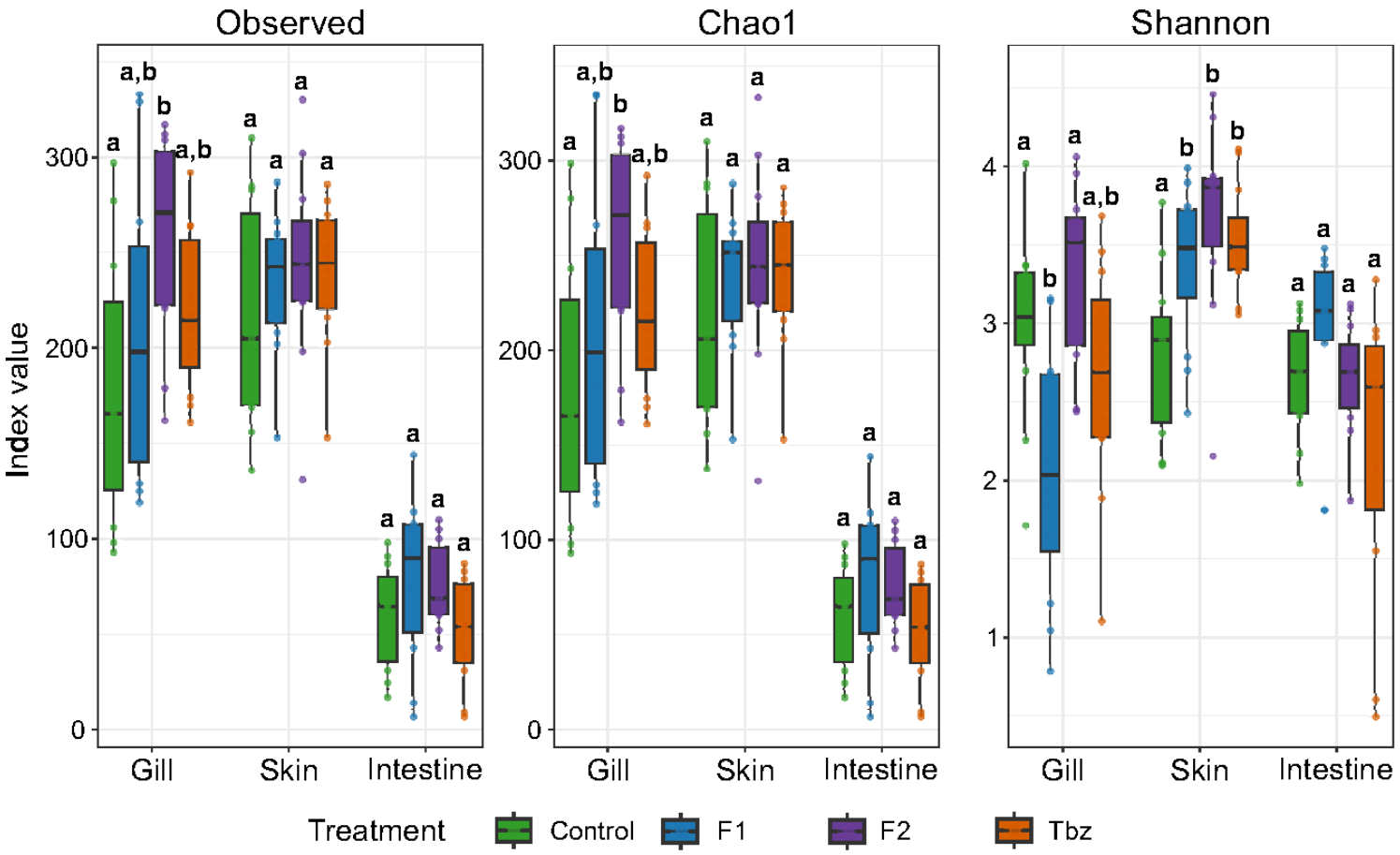

Figure 1

Alpha diversity per tissue and treatment. Alpha diversity was quantified using three indexes (left to right): Observed, Chao1 and Shannon. Measures were calculated after exposure for 7 months to different treatments (coloured boxplots): fluoride (F1, 6.8 mg F-/L or F2, 24.7 mg F-/L), tebuconazole (Tbz, 51.7 µg/L) or a control condition. Statistical comparisons were performed for each tissue independently, different letters indicate significant differences among treatments ($p < 0.05$).

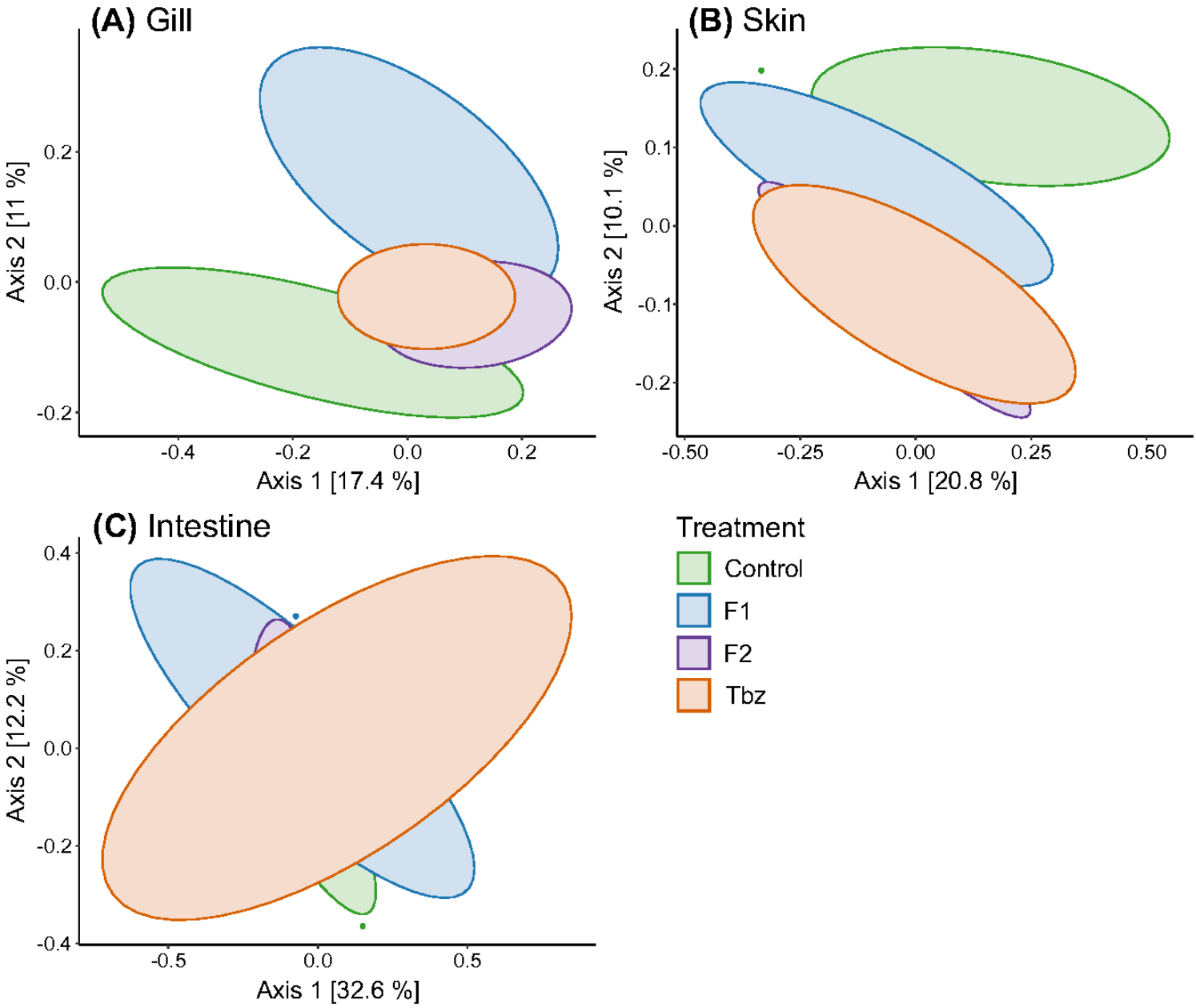

Figure 2

Principal Coordinates Analysis (PCoA) based on Bray-Curtis dissimilarity matrices. PCoA are displayed for (A) gill, (B) skin and (C) intestine samples. Points represent individual samples and are coloured according to treatment. Ellipses represent 95% confidence intervals around group centroids based on a multivariate t-distribution. Percentages on the axes indicate the proportion of variance explained by each principal coordinate. Data were normalized using cumulative sum scaling (CSS) prior to ordination.

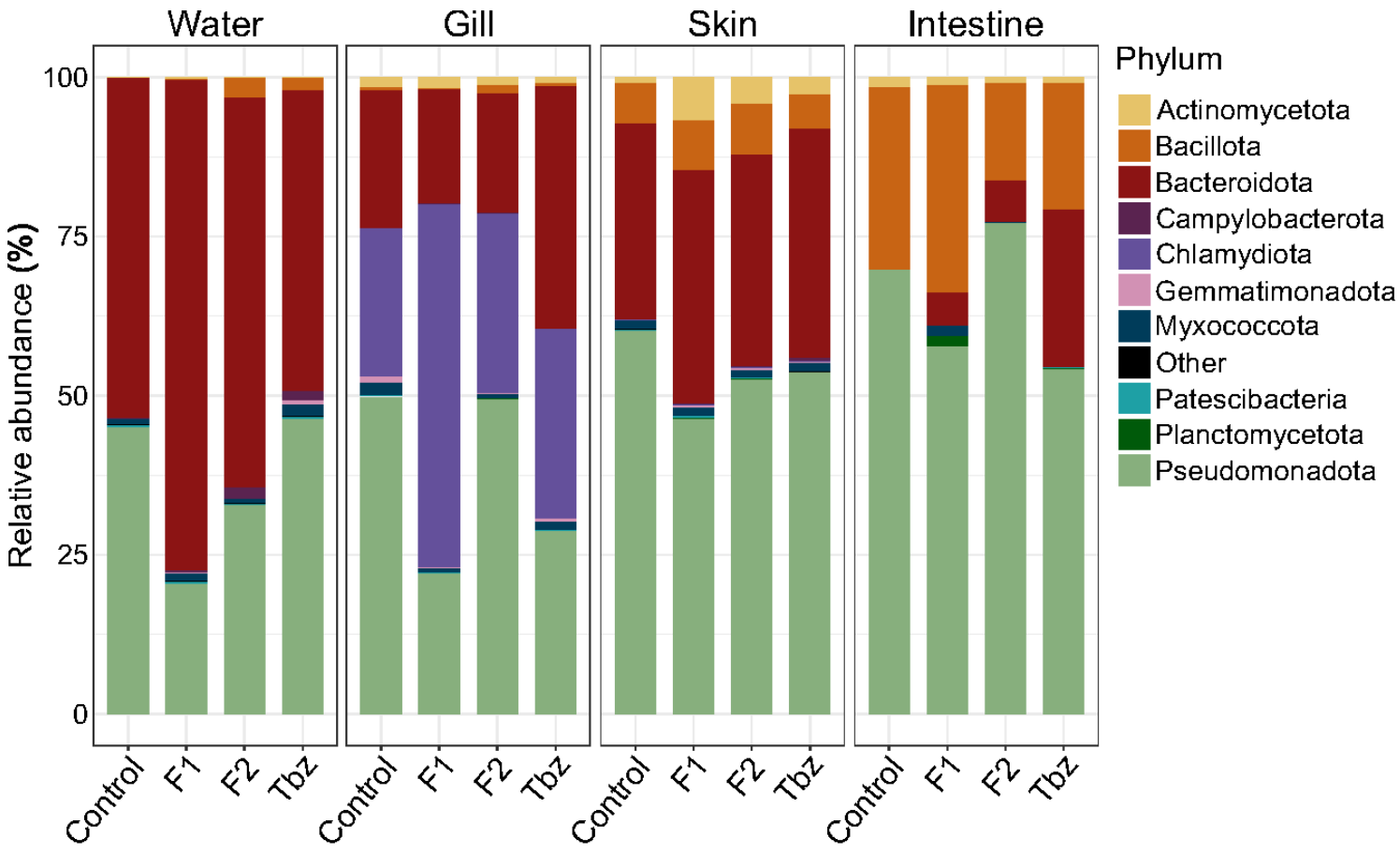

Figure 3

Taxonomical composition at the phylum level. Relative abundance of the 10 dominant phyla by sample type and treatment. Remaining phyla are grouped under “Other”.

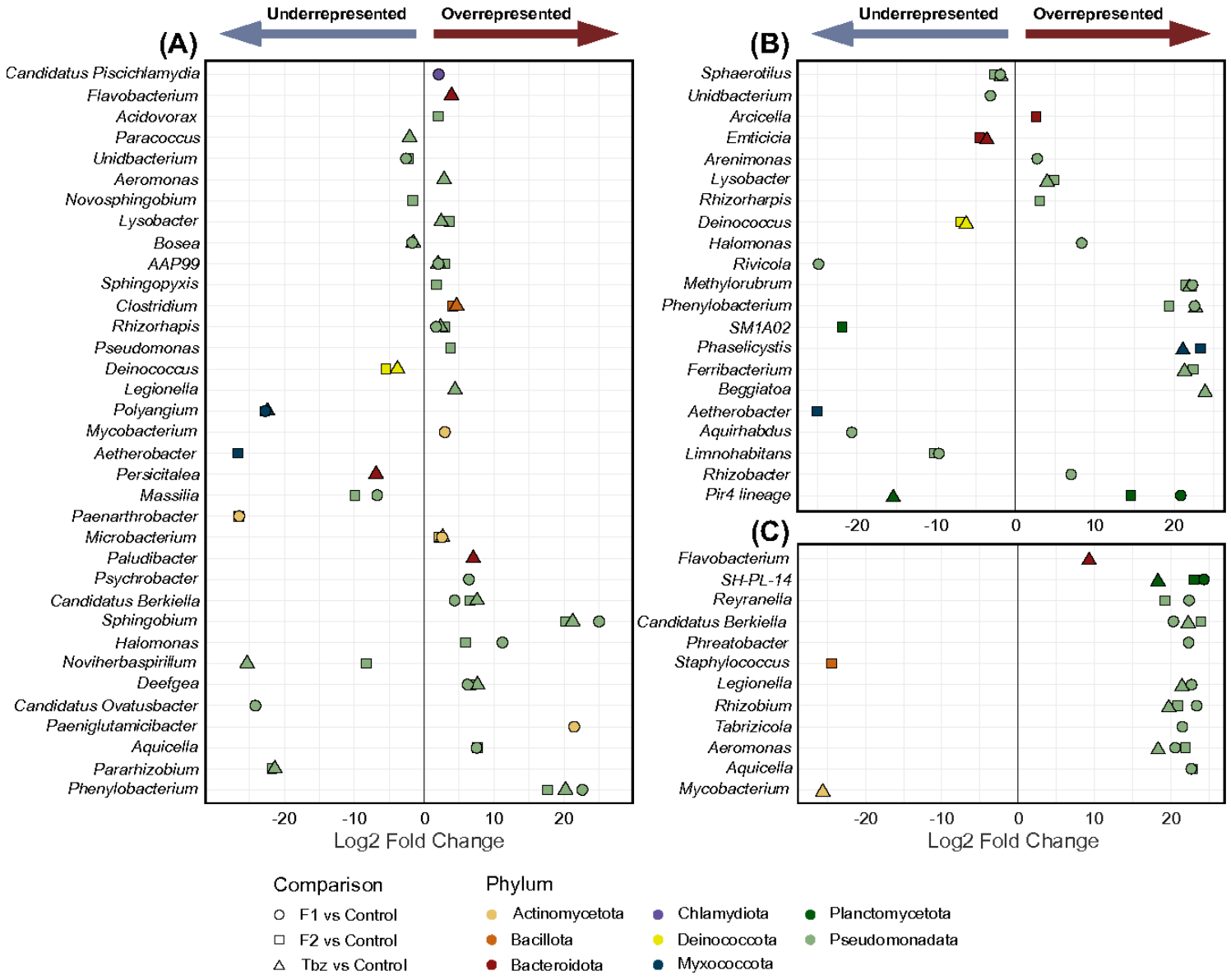

Figure 4

Differential analysis results. Differential analyses were performed at the genus level using DESeq2. Genera showing significantly different abundances between at least one treatment condition, and the control (p-value < 0.01), are displayed for gill (A), skin (B) and intestine (C) samples. Genera are ordered by decreasing mean relative abundance (top to bottom). The shape of the points indicates the between-treatments comparison pair, while their colour corresponds to the phylum.

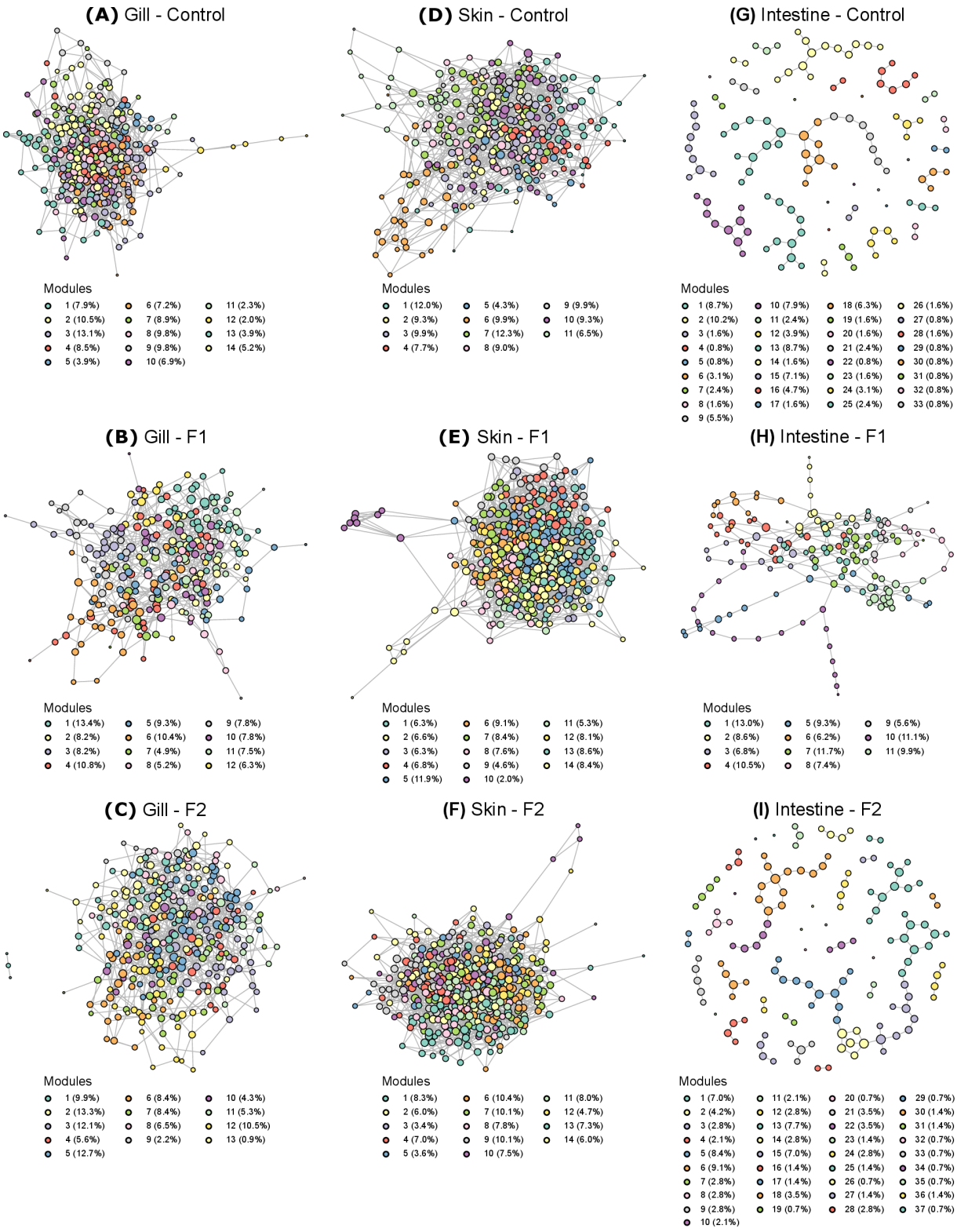

Figure 5

Microbial co-occurrence networks. Networks are displayed in the gill (A – C), skin (D – F) and intestine (G – I) samples under control (A, D, G), F1 (B, E, H) and F2 (C, F, I) treatment conditions. Co-occurrence networks were inferred using SPIEC-EASI and modules were detected with the Louvain algorithm. Each coloured node represents an ASV; node colour indicates its membership to a network module, i.e., a group of highly interconnected ASVs. The percentage of ASVs assigned to each module is reported in

the legend. Grey edges indicate significant co-occurrences between two nodes. Edge length is determined solely by the two-dimensional layout (Fruchterman-Reingold) and does not represent the strength nor distance of associations. Node size is proportional to the number of edges (node degree).

Supplementary Files

This is a list of supplementary files associated with this preprint. Click to download.

- Additionalfile1.pdf
- Additionalfile2.pdf
- Additionalfile3.xls
- Additionalfile4.xls
- Additionalfile5.xls
- Additionalfile6.xls